1972

Determination of thermal contact resistance between metals using a pulse technique

William Edward Stewart Jr.

Department: Mechanical and Aerospace Engineering

DETERMINATION OF THERMAL CONTACT RESISTANCE BETWEEN METALS USING A PULSE TECHNIQUE

by

WILLIAM EDWARD STEWART, JR. 1944-

A DISSERTATION

Presented to the Faculty of the Graduate School of the

UNIVERSITY OF MISSOURI-ROLLA

In Partial Fulfillment of the Requirements for the Degree

DOCTOR OF PHILOSOPHY

in

MECHANICAL ENGINEERING

1972

Harry L. Stanley Jr. — Advisor
J. A. Jarrett
C. G. Remington
R. J. Perrico
A. K. Rigler
T. S. Chen

ABSTRACT

This dissertation reports the results of an experimental and analytical investigation to determine the thermal contact resistance of several metal specimen pairs using a relatively new pulse technique. Metal specimens were aluminum 2024-T3, aluminum 6061-T6, aluminum 7075-T6, copper 110, stainless steel 304, molybdenum, and Armco iron. Thermal contact resistance was also determined for dissimilar metal specimen pairs of aluminum 6061-T6 - copper 110 and aluminum 7075-T6 - copper 110. Aluminum 7075-T6, copper 110, and stainless steel 304 specimens were tested to determine the variance of contact resistance with time after loading.

Specimens were circular cylindrical disks between .033 and .061 inches thick and .788 inches in diameter. Specimen contacting surfaces were nominally flat and polished to a surface rms roughness of approximately 2 micro-inches. Axial loads were applied from 20.7 to 124.2 psi in a 10 micron (10^{-5}mm Hg) vacuum and -10°F environment.

Results of the experiments showed that the thermal contact resistance decreased with increasing load,

decreased with increasing time after initial loading and that directional effects are probably not a result of differential thermal expansion and the directional effect exists at relatively low interface pressures.

Thermal contact resistance decreased approximately 40 percent for aluminum 2024-T3 and aluminum 6061-T6 specimens. Aluminum 7075-T6 specimens decreased approximately 75 percent in thermal contact resistance over the interface pressure range of 20.7 to 124.2 psi. Molybdenum values of thermal contact resistance closely approximate those of aluminum 2024-T3 and aluminum 6061-T6 with a 62 percent decrease over the same pressure range.

Copper 110 specimen data were approximately 50 percent less than the aluminum 2024-T3 and aluminum 6061-T6 data and decreased about 43 percent over the pressure range tested, while Armco iron and stainless steel data had approximately four and five times the values of thermal contact resistance as those obtained for aluminum 2024-T3 and aluminum 6061-T6 specimens.

Data obtained from experiments to determine the decrease in thermal contact resistance after initial loading indicated approximately 9 to 66 percent decreases in contact resistance. Variances between thermal contact resistances for directional effects

experiments were on the order of 20 percent.

Correlation between aluminum specimen thermal contact resistance data of this and other investigations is discussed.

ACKNOWLEDGEMENT

The author is indebted to Dr. Harry J. Sauer, Jr. for his guidance and advice during this investigation and also for providing the opportunity to perform the experiments.

The author also wishes to thank Dr. Thomas Faucett, Chairman of the Mechanical and Aerospace Engineering Department, for making available the Graduate Teaching Assistantships which has made all of this financially possible, and Mr. Ken Mirly for assistance in equipment preparation.

And, finally, the author wishes to express his fond appreciation to his wife, Linda, for her encouragement and sacrifice through these long years of studying and for her genius at budgeting our financial impoverishment.

TABLE OF CONTENTS

Table of Contents (continued) Page

LIST OF ILLUSTRATIONS

List of Illustrations (continued)

LIST OF TABLES

I. INTRODUCTION

The area of study of heat transfer at the interface of two materials in contact has in recent years been of increasing interest. When two surfaces are brought into contact the actual contacting area between the two surfaces is actually only a small part of the total apparent contact surface area and is generally between one and ten percent.

This imperfect contact between the two surfaces as shown in Figures 1 and 2 consist of both macroscopic and microscopic contacts. Macroscopic contacts are directly dependent on the flatness or waviness of the surfaces in contact and also the degree of surface roughness. Where macroscopic contact exists the effect of microscopic contact becomes dominant. The degree of microscopic contact depends upon the surface roughness and hardness.

The imperfect contact at the interface when subjected to a heat flux results in a temperature discontinuity. The flux lines in passing between the two metals tend to converge at the points of solid-to-solid contact. This is due to the higher thermal conductivity, and hence lower resistance to heat flow, of the metal-to-metal contacts than of the void areas around the contacts, whether they are filled with air or in a vacuum. A resistance to heat flow produced by this constriction of heat flux lines through these small contacts and the temperature discontinuity results since in effect the heat flow is "delayed" from crossing the interface.

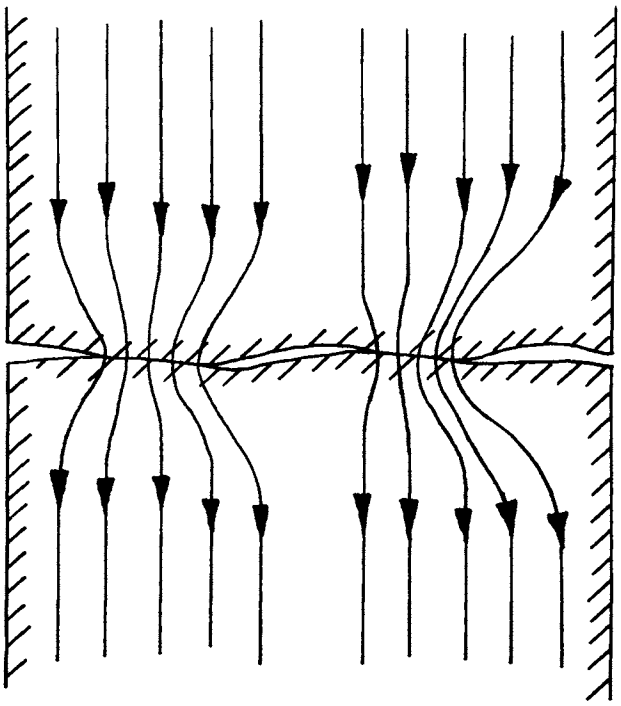

Macroscopic Constriction of Heat Flow

Figure 1

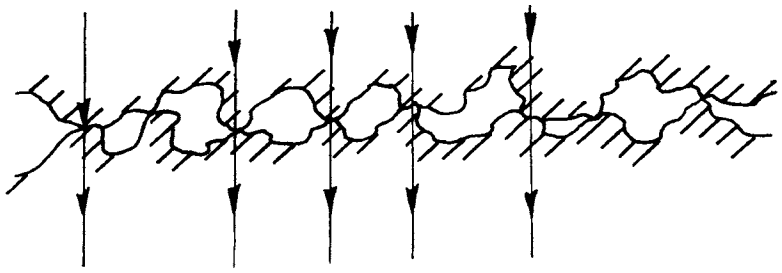

Microscopic Constriction of Heat Flow

Figure 2

This resistance to heat transfer across the interface is defined by

$$R = \frac{(A)(\Delta T)}{Q}$$

where R = thermal contact resistance, Btu/ Hr Sq Ft F

A = apparent contact surface area, Sq Ft

ΔT = temperature drop across the interface, F

Q = heat flow rate across the interface, Btu/Hr

The thermal contact resistance is then a function of the temperature level and the apparent contact interface pressure or load since at higher interfacial pressures elastic and plastic deformation will occur creating greater solid-to-solid contact area.

A single perfect contact over part of the apparent contact area is usually considered by analytical approaches to the problem of thermal contact resistance. This approach is somewhat hampered in relating to actual contacts by surface contamination and the formation of oxide layers on the surfaces of the contacting metals. Most oxide layers have lower thermal conductivities than the metal itself and while analytical methods are based upon the radius of the perfect contact, the actual contact is area dependent.

Therefore it is clear that the condition of the surfaces in contact be defined as clearly as possible.

In order for thermal contact resistance to be of value the surface roughness, relative flatness, hardness, and state of oxidation must be defined.

Practical applications of the results of thermal contact resistance studies demand that these surface parameters be defined. In recent years many practical problems have relied upon thermal contact resistance data. As Minges (1)* states, there are several areas of interest that must deal with the problem of restrictions of heat flow. Aircraft structures are subjected to high heat loads at hypersonic speeds and contact resistance between structural members must be known. High temperature turbines must dissipate heat across many components with surfaces in contact. Also in the space programs, manned vehicles must be precisely temperature controlled in a vacuum environment and interfacial heat transfer is a major design consideration. Fuel elements for nuclear reactors are plated with a low neutron absorption alloy. Due to high heat flows the thermal contact resistance between even good contact of fuel elements and plating can be large.

As noted previously the thermal contact resistance between two metal surfaces is a function of the metal

* Parentheses refer to listings in Bibliography

material itself, the surface roughness and hardness, the surface flatness, and the apparent contact pressure. These are the contributing factors to the effective metal-to-metal contact area, as noted by Fried and Costello (2).

The concept that the contact area is actually only a few discrete points was also presented by Fenech and Rohsenow (3) and they noted that heat flow will channel through these few points in contact. They considered radiation and convection to be negligible in the interstitial gas between the metal surfaces for low temperature.

One of the first studies of contact resistance was carried out by Cetinkale and Fishenden (4). They assumed that the heat flux lines were parallel to the specimen axis and converged to the contact points as the interface was approached. This was the result of the assumption that the thermal conductivity of the contact points was much greater than the interstitial gas. They also assumed that as the contact pressure was increased, the contact points of the softer material will plastically deform until the pressure at the contact point is equal to its Meyer hardness. For other than ground surfaces their test data on steel, brass, and aluminum contacts were not consistent

with the theoretical formulation.

When two surfaces are in contact in an atmospheric environment, the interfaces are largely separated by air. The ratio of the thermal conductivity of air to that of a good metallic conductor is of the order 1 to 10^4, as noted by Powell (5), which lends further substance to the idea that the essential means of heat transfer at the interfaces of metal surfaces is a result of metal-to-metal contacts.

In other investigations it has been shown that there is only a small difference between contact resistance with air as the interstitial medium and with the voids evacuated. Petri (6) showed that for aluminum - molybdenum specimen pairs the contact resistance varied as little as 7.2 percent less at a vacuum environment of 10^{-5}mm Hg as compared to an atmospheric air environment at constant pressures of 140 psi. Primary transport of heat was then concluded to be through the solid contacts.

Investigations have been performed on the determination of the effect of interstitial materials on the thermal contact resistance of metals in contact. Koh and John (7) concluded that in using foils between the interfaces of metal specimens the softness of the foil material rather than its thermal conductivity

is of prime importance. The softer the material, the greater tendency it has to fill the gaps around the contact points. Experiments by Barzelay, Tong, and Holloway (8) showed that foils placed at the interface of metals also decreases the contact resistance appreciably and that thermal resistance decreases with increasing mean interface temperature but remains relatively constant at different heat flow rates. In further investigations by Barzelay, et al (9), it was noted that as the interface pressure is increased the thermal resistance of interfaces decrease. This dependence upon apparent contact pressure was more pronounced for softer materials. They also noted that as the temperature levels were increased, the thermal resistance increased owing to the assumption that at higher temperatures the interfaces tend to warp, breaking metal-to-metal contacts.

Other investigations were made to find the effect of interstitial materials on the thermal contact resistance. Fletcher, Smuda, and Gyorog (10) tested several materials to determine those most suitable for increasing the interface resistance. Cloth felt provided the best insulation while silicone greases provided the least thermal resistance of the interstitial materials tested which included gold

leaf and indium foil which have high thermal conductivities. Sauer, Remington, Stewart, and Lin (11) tested aluminum and stainless steel specimens using stainless steel screens of varying mesh size, paper, aluminum foil, and silicone greases as interstitial materials. They found that silicone greases and aluminum foil greatly decrease the contact resistance relative to bare contacts since these materials tend to fill the voids between the surfaces of the specimens. Stainless steel screens on the other hand greatly increase the thermal contact resistance due to a greatly decreased number of metal-to-metal contacts.

Under transient temperature conditions Barzelay, et al, (12) concluded that the thermal resistance may vary considerably from specimen to specimen and from test to test on the same specimen. Barzelay (13) later also noted that the interface resistance may vary considerably for essentially identical specimens but this may have been due to poorly defined surface configuration.

Surface hardness affects the degree of contact resistance. Shlykov and Gamin (14) observed that heat transfer primarily takes place at points of contact for softer metals while for hard metals heat transfer

also takes place to a relatively significant extent through the interstitial gas.

Since those first experimental methods of contact resistance of metallic contacts more sophisticated experimental and analytical approaches to the problem have been made. This has been performed to increase the amount of available data on actual surface contacts of metals and to try to predict the means and mechanisms of contact resistance on a macroscopic and microscopic basis.

Thomas and Probert (15) advanced a theory to explain the theoretical basis of heat transfer at interfaces both on a macroscopic and microscopic basis. They correlated the results of many experiments by other investigators as the results related to specimen material, surface roughness, surface hardness, mean interface temperature, thermal conductivity, and interstitial material. They concluded, though, that from the correlated results the theory, based upon the basic approach of contact resistance being inversely proportional to the thermal conductivity and the radius of a perfect contact, fails to predict the experimental results and suggest that surface finish variations from specimen to specimen and from investigator to investigator are the probable cause for variations from the predicted theory, and also

between experiments.

Similar correlations were carried out by Veziroglu (16) on experimental results of several researchers and gave a procedure for estimating the thermal contact resistance based on the correlations. The analysis considered such parameters as contact materials, interstitial fluids, surface finishes, contact pressures, and temperatures. Results shown give a reasonable approximation to experimental data.

Analytical predictions of thermal contact resistance are usually based upon the particular metals in contact, contact pressure, and the surface conditions for macroscopic investigations. For microscopic investigations the parameters of study are usually based upon contact geometry including many assumptions as to the surface profiles and the distribution of actual contacts.

Cooper, Mikic, and Yovanovich (17) considered two solid metal bodies in contact in a vacuum. They theoretically predicted the thermal contact resistance based upon typical profiles of mating surfaces and deformation theory. Their prediction agreed well with their comparison to a few experimental results. An investigation by Holm (18) was based upon two dimensionless parameters which were functions of the

particular metal and of the total applied load (the apparent contact load). His approach was substantiated by comparison with several experimental results.

Thomas and Probert (19) continued the study of Holm and considered further the surface hardness and roughness using a dimensional analysis. They obtained results which more closely predicted the results than did Holm's work when compared to results from several experiments.

Mikic and Carnasciali (20) described an analytical prediction of the thermal contact conductance of stainless steel plated with a thin sheet of copper. Their experimental results agreed with their prediction using the perfect single contact method and noted that the copper plating reduces the contact resistance by an order of magnitude. This investigation was essentially another study of the effect of an interstitial material since the copper, being more ductile than stainless steel, tended to fill the voids more easily at the interface contact than would a stainless steel interface alone and thereby decreased the thermal contact resistance.

Due to heat flow being directed through the relatively small metal-to-metal contact points at the interface of two surfaces in contact, there exists

a non-uniform temperature across the surface and to which may result in thermal stresses and warpage of the surfaces. Rogers (21) reported that there is less contact resistance when heat flows from aluminum to steel than from steel to aluminum. This phenomenon is referred to as the directional effect of dissimilar metals in contact.

An explanation of the directional effect was set forth on a macroscopic and microscopic basis by Clausing and Chao (22) and later in more detail by Clausing (23). They tried to predict the results of the directional dependence of heat flow and concluded that the thermal strain caused by the temperature differences at the interface influences the differences in contact resistance. Also it was shown that thermal contact resistance is less for heat flows from stainless steel to aluminum which was exactly opposite to the results of Rogers. Their results were based primarily on macroscopic (flatness) approach as in contrast to the microscopic (roughness) approach used by Yovanovich and Fenech (24). Their study considered rough surfaces and obtained good agreement between theory and experiment.

Lewis and Perkins (25) reported that the directional effect was dependent upon the interface surface

conditions of roughness and flatness. Hence they considered both the microscopic and macroscopic approach to explain the directional effect. They predicted the results of Clausing's macroscopic approach for specimens of flatnesses varying from 90 to 2000 micro-inches, or that contact resistance was less when heat flow was from stainless steel to aluminum. They also predicted the results of Barzelay, et al, (9) by a microscopic approach for rough specimens, or that contact resistance is less when heat flow was from aluminum to stainless steel.

Thomas and Probert (26) also considered the dependence of the thermal contact resistance upon the direction of heat flow for similar and dissimilar metal specimen pairs. Their study was based on the thermal conductivity, surface hardness, the surface rms roughness, and the mean surface slope of the contact surfaces in predicting thermal contact resistance. Even though their theory closely approximates the experimental results for similar metals, the theory does not predict accurately the directional effect between dissimilar metals.

In recent years new experimental techniques to determine the thermal properties of metals have been explored. Parker, Jenkins, Butler, and Abbott (27)

proposed a technique for measuring the thermal diffusivity, heat capacity, and thermal conductivity of materials using a high-intensity, short-duration pulse of radiant energy through the use of a Xenon flash tube. The radiant energy or light impinges upon the front surface of a specimen and the temperature rise history is measured on the back surface. Through the manipulation of an equation given by Carslaw and Jaeger (28) with the appropriate boundary conditions and the recorded temperature history, the thermal properties can be found. Their results for several metals were within a few percent error of previously published values.

Extensions of the approach by Parker, et al, were carried out by Cowan (29) and Larson and Koyana (30) which were a more generalized approach to the measurement of the thermal properties taking into account radiation losses, effects of flash duration, and other more subtle considerations. They also considered variations on the initial experimental techniques for measurements at high temperatures.

Other pulse heating techniques such as the work by Danielson (31) have increased the amount of available experimental results for comparative purposes.

Studies of transient heat flow between solid materials in contact and their usefulness in predicting

thermal contact resistance have received less attention. An experimental pulse-heating technique offers several advantages over the more common steady-state experimental techniques as used previously by most investigators. A short-duration experiment would allow the determination of thermal contact resistance with time after initial loading of specimens and have the advantage of rapid accumulation of data. Steady-state techniques usually require one to two days to reach an equilibrium point. Laurent and Sauer (32) reported a transient technique to measure thermal contact resistance also using a flash method. Moore and Blum (33) also used a transient technique to measure thermal contact resistance.

In an effort to present a valuable amount of data on thermal contact resistance using a relatively new technique and to try to resolve a few uncertainties concerning the directional effect dependence on heat flow rates, this investigation was undertaken.

II. MATHEMATICAL ANALYSIS

As shown in Figure 3, two metal specimens are in contact at x=0. The left hand specimen is x_1 in length with thermalconductivity k_1 and thermal diffusivity is α_1. The right hand specimen is x_2 in length with thermal conductivity k_2 and thermal diffusivity is α_2.

When the specimens are subjected to an instantaneous pulse input of energy at $x=-x_1$, the heat transfer through the two specimens is assumed to be one-dimensional time dependent. The governing partial differential equations for specimens 1 and 2 are then

$$\frac{\partial^2 T_1(x,t)}{\partial x^2} = \frac{1}{\alpha_1} \frac{\partial T_1(x,t)}{\partial t} \tag{1}$$

and

$$\frac{\partial^2 T_2(x,t)}{\partial x^2} = \frac{1}{\alpha_2} \frac{\partial T_2(x,t)}{\partial t} \quad . \tag{2}$$

Both specimens are subjected to a vacuum environment and therefore the assumption is made that there is no convection heat transfer at all exterior surfaces. Also radiation effects are considered to be negligible for the low temperature environments after the face at $-x_1$ initially receives an instantaneous

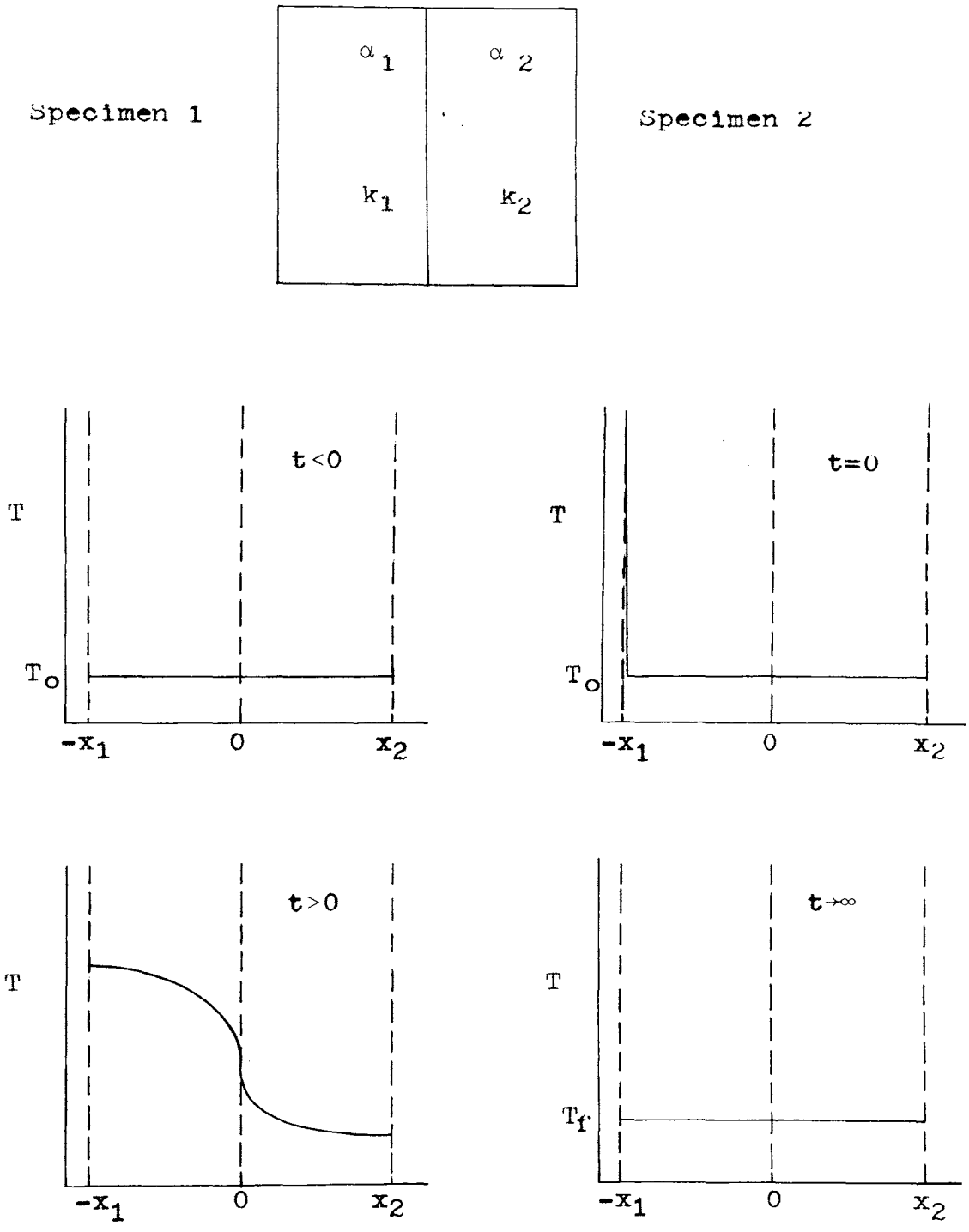

Schematic Diagram of Specimens in Contact

Figure 3

radiative input such that,

$$\frac{\partial T_1}{\partial x}(-x_1,0) = \frac{q_0}{k_1} \quad ,$$

where q_0 is the radiant energy input. However, since q_0 is not generally known, the following method has been developed to circumvent this unknown. Using the forementioned assumptions the following boundary conditions apply to the specimens in contact.

1) $$k_1\frac{\partial T_1(-x_1,t)}{\partial x} = 0, \quad t>0 \tag{3}$$

2) $$k_2\frac{\partial T_2(x_2,t)}{\partial x} = 0, \quad t>0 \tag{4}$$

3) $$k_1\frac{\partial T_1(0-,t)}{\partial x} = k_2\frac{\partial T_2(0+,t)}{\partial x} \tag{5}$$

Boundary conditions 1) and 2) signify no heat losses from surfaces at $-x_1$ and x_2. Boundary condition 3) signifies that the heat transfer from specimen 1 must equal the heat transfer to specimen 2 at x=0. Also at the contact surface, the thermal contact resistance, R, is defined to be the ratio of the temperature drop across the interface to the heat transfer across it. Then

4) $$k_1\frac{\partial T_1(0-,t)}{\partial x} = \left(\frac{1}{R}\right)(T_2(0+,t)-T_1(0-,t)) \; . \tag{6}$$

Also since the two specimens are in intimate

contact the rate of heat transfer from specimen 1 must be equal to the rate of heat transfer to specimen 2. Then

5) $$\frac{\partial}{\partial t}\left(\frac{k_1 \partial T_1(0-,t)}{\partial x}\right) = \frac{\partial}{\partial t}\left(\frac{k_2\ T_2(0+,t)}{\partial x}\right) \quad . \tag{7}$$

Using the method of separation of variables to solve equations (1) and (2), let

$$T(x,t) = X(x)Z(t) \tag{8}$$

then

$$Z\frac{d^2X}{dx^2} = \frac{1}{\alpha} X \frac{dZ}{dt} \quad . \tag{9}$$

or

$$\frac{1}{X}\frac{d^2X}{dx^2} = \frac{1}{\alpha Z}\frac{dZ}{dt} = -\lambda^2 \quad . \tag{10}$$

Therefore

$$\frac{d^2X}{dx^2} + \lambda^2 X = 0 \quad , \tag{11}$$

$$\frac{dZ}{dt} + \alpha\lambda^2 Z = 0 \quad . \tag{12}$$

Therefore the solution becomes

$$T(x,t) = \sum_{n=1}^{\infty} (A_n \cos\lambda_n x + B_n \sin\lambda_n x)e^{-\alpha\lambda_n^2 t} + C_n \quad . \tag{13}$$

Only one λ is generally significant and need be determined when obtained where the shape of the

temerature history is strongly dependent upon the thermal contact resistance. However the validity of this assumption rests with the shape of the actual recording. Then

$$T(x,t) = (A \cos \lambda x + B \sin \lambda x)e^{-\alpha\lambda^2 t} + C \quad , \qquad (13a)$$

which is the sum of the transient and steady state parts. Then for each specimen, let

$$T_1(x,t) = (A_1 \cos \lambda_1 x + B_1 \sin \lambda_1 x)e^{-\alpha_1 \lambda_1^2 t} + C \qquad (14)$$

and

$$T_2(x,t) = (A_2 \cos \lambda_2 x + B_2 \sin \lambda_2 x)e^{-\alpha_2 \lambda_2^2 t} + C \quad . \qquad (15)$$

Application of the boundary conditions then yields the following results:

$$\text{from B.C. 1), } k_1 \frac{\partial T_1(-x_1,t)}{\partial x} = 0, \text{ equation (14)}$$

becomes

$$-k_1(-A_1\lambda_1 \sin \lambda_1(-x_1) + B_1\lambda_1 \cos \lambda_1(-x_1))e^{-\alpha_1 \lambda_1^2 t} = 0$$

or

$$A_1 = \frac{-B_1 \cos \lambda_1 x_1}{\sin \lambda_1 x_1} = -B_1 \cot \lambda_1 x_1 \qquad (16)$$

$$\text{from B.C. 2), } k_2 \frac{\partial T_2(x_2,t)}{\partial x} = 0, \text{ equation (15) becomes}$$

$$k_2(-A_2\lambda_2 \sin \lambda_2 x_2 + B_2\lambda_2 \cos \lambda_2 x_2)e^{-\alpha_2\lambda_2^2 t} = 0$$

or

$$A_2 = B_2 \cot \lambda_2 x_2 \tag{17}$$

from B.C. 3), $k_1 \frac{\partial T_1(0-,t)}{\partial x} = k_2 \frac{\partial T_2(0+,t)}{\partial x}$,

equations (14) and (15) become

$$k_1 e^{-\alpha_1\lambda_1^2 t}(-A_1\lambda_1 \sin \lambda_1 0- + B_1\lambda_1 \cos \lambda_1 0-)$$

$$= k_2 e^{-\alpha_2\lambda_2^2 t}(-A_2\lambda_2 \sin \lambda_2 0+ + B_2\lambda_2 \cos \lambda_2 0+)$$

or

$$B_1\lambda_1 k_1 e^{-\alpha_1\lambda_1^2 t} = B_2\lambda_2 k_2 e^{-\alpha_2\lambda_2^2 t} \tag{18}$$

from B.C. 4), $k_1 \frac{\partial T_1(0-,t)}{\partial x}$

$$= \left(\frac{1}{R}\right)(T_2(0+,t) - T_1(0-,t)) ,$$

and from equations (14) and (15) it follows that,

$$k_1 \frac{\partial T_1(0-,t)}{\partial x}$$

$$= k_1(-A_1\lambda_1 \sin \lambda_1(0-) + B_1\lambda_1 \cos \lambda_1(0-))e^{-\alpha_1\lambda_1^2 t}$$

$$= k_1 B_1 \lambda_1 e^{-\alpha_1 \lambda_1^2 t}$$

$$T_2(0+,t) = (A_1 \cos \lambda_1(0+) + B_1 \sin \lambda_1(0+))e^{-\alpha_1 \lambda_1^2 t} + C$$

$$= A_1 e^{-\alpha_1 \lambda_1^2 t} + C$$

$$T_2(0+,t) = (A_1 \cos \lambda_1(0+) + B_1 \sin \lambda_1(0+))e^{-\alpha_1 \lambda_1^2 t} + C$$

$$= A_1 e^{-\alpha_1 \lambda_1^2 t} + C$$

and then

$$k_1 B_1 \lambda_1 e^{-\alpha_1 \lambda_1^2 t} = (\tfrac{1}{R})(A_2 e^{-\alpha_2 \lambda_2^2 t} - A_1 e^{-\alpha_1 \lambda_1^2 t}) \qquad (19)$$

Solving for R, the thermal contact resistance,

$$R = \frac{A_2 e^{-\alpha_2 \lambda_2^2 t} - A_1 e^{-\alpha_1 \lambda_1^2 t}}{k_1 B_1 \lambda_1 e^{-\alpha_1 \lambda_1^2 t}} \qquad (20)$$

Using equations (16), (17), and (18), equation (20) can be simplified by substituting for A_1 and A_2

$$R = \frac{(B_2 \cot \lambda_2 x_2) e^{-\alpha_2 \lambda_2^2 t} - (-B_1 \cot \lambda_1 x_1) e^{-\alpha_1 \lambda_1^2 t}}{k_1 B_1 \lambda_1 e^{-\alpha_1 \lambda_1^2 t}}$$

$$R = \left(\left(B_1 \frac{\lambda_1 k_1 e^{-\alpha_1 \lambda_1^2 t}}{2 k_2 e^{-\alpha_2 \lambda_2^2 t}} \cot \lambda_2 x_2 \right) e^{-\alpha_2 \lambda_2^2 t} + (B_1 \cot \lambda_1 x_1) e^{-\alpha_1 \lambda_1^2 t} \right) /$$

$$(k_1\lambda_1 B_1 e^{-\alpha_1\lambda_1^2 t})$$

$$= \frac{\frac{\lambda_1 k_1}{\lambda_2 k_2}\cot\lambda_2 x_2 + \cot\lambda_1 x_1}{k_1\lambda_1}$$

$$R = \frac{\cot\lambda_1 x_1}{k_1\lambda_1} + \frac{\cot\lambda_2 x_2}{k_2\lambda_2} \qquad (21)$$

Using B.C. 5),

$$\frac{\partial}{\partial t}\left(k_1 \frac{\partial T_1(0-,t)}{\partial x}\right) = \frac{\partial}{\partial t}\left(k_2 \frac{\partial T_2(0+,t)}{\partial x}\right)$$

yields

$$k_1 B_1 \lambda_1(-\alpha_1\lambda_1^2)e^{-\alpha_1\lambda_1^2 t} = k_2 B_2\lambda_2(-\alpha_2\lambda_2^2)e^{-\alpha_2\lambda_2^2 t}$$

however from B.C. 3), it is known that

$$k_1 B_1 \lambda_1 e^{-\alpha_1\lambda_1^2 t} = k_2 B_2\lambda_2 e^{-\alpha_2\lambda_2^2 t}$$

therefore the following relation exists,

$$\alpha_1\lambda_1^2 = \alpha_2\lambda_2^2$$

or

$$\lambda_2 = \lambda_1\sqrt{\frac{\alpha_1}{\alpha_2}} \qquad (22)$$

Substitution of equation (22) into equation (21) yields the final form for the thermal contact resistance R.

$$R = \frac{\cot \lambda_1 x_1}{k_1 \lambda_1} + \frac{1}{k_2 \lambda_1}\sqrt{\frac{\alpha_2}{\alpha_1}} \cot\left(\lambda_1\sqrt{\frac{\alpha_1}{\alpha_2}}\, x_2\right) \qquad (23)$$

where λ_1 is the only unknown.

With the assumption that there is a first order exponential temperature history at $x=x_2$ on specimen 2, then equation (15) becomes as before,

$$T_2(x_2,t)$$

$$= \left(A_2\cos \lambda_1\sqrt{\frac{\alpha_1}{\alpha_2}}\, x_2 + B_2\sin \lambda_1\sqrt{\frac{\alpha_1}{\alpha_2}}\, x_2\right)e^{-\alpha_1\lambda_1^2 t} + C. \qquad (24)$$

For simplification, let

$$D = A_2\cos \lambda_1\sqrt{\frac{\alpha_1}{\alpha_2}}\, x_2 + B_2\sin\lambda_1\sqrt{\frac{\alpha_1}{\alpha_2}}\, x_2,$$

then equation (24) becomes

$$T_2(x_2,t) = De^{-\alpha_1\lambda_1^2 t} + C \qquad (25)$$

which agrees with the equation for the actual or experimentally determined history at x_2.

A typical temperature history as a function of time is shown in Figure 4, where the initial temperature at x_2 is zero and its final temperature is a constant, T_f.

From Figure 4 it can be seen that as t approaches infinity, the temperature at $x=x_2$ is the constant temperature T_f, therefore

$$C = T_f \, . \qquad (26)$$

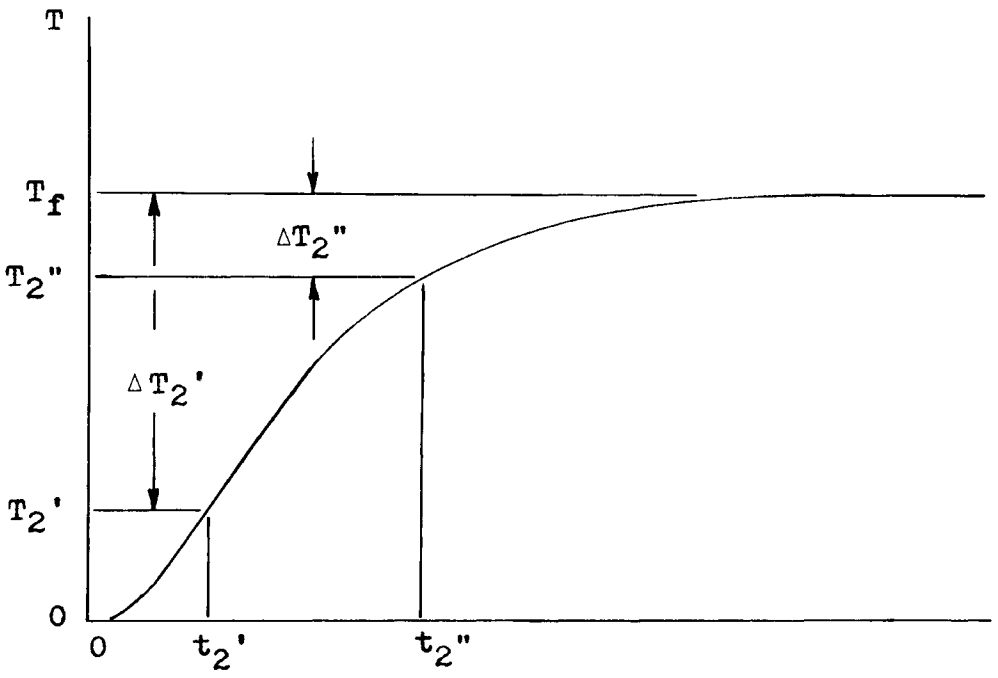

Typical Temperature History Recording at $x=x_2$

Figure 4

Also at t=0, the temperature at $x=x_2$ is zero, and therefore

$$D = -T_f \quad . \tag{27}$$

Then equation (25) becomes

$$T_2(x_2,t) = T_f - T_f e^{-\alpha_1 \lambda_1^2 t} \quad . \tag{28}$$

For any random time t_2', $0<t_2'<t_f$, and any time t_2'', $0<t_2'<t_2''<t_f$, the corresponding temperature at $x=x_2$ becomes

$$T_2(x_2,t_2') = T_f - T_f e^{-\alpha_1 \lambda_1^2 t_2'} \tag{29}$$

and

$$T_2(x_2,t_2'') = T_f - T_f e^{-\alpha_1 \lambda_1^2 t_2''} \quad , \tag{30}$$

where

$$T_2' = T_2(x_2,t_2') \text{ and } T_2'' = T_2(x_2,t_2'') \quad .$$

Let,

$$\Delta T_2' = T_f - T_2' \text{ and } \Delta T_2'' = T_f - T_2''$$

then from equations (29) and (30)

$$T_2' = T_f e^{-\alpha_1 \lambda_1^2 t_2'}$$

and

$$T_2'' = T_f e^{-\alpha_1 \lambda_1^2 t_2''}$$

For convenience of calculation, select

$$\Delta T_2'' = \frac{\Delta T_2'}{e} . \qquad (31)$$

Then after the selection of time t_2', the corresponding time t_2'' can be determined.

It follows from equation (31) then, that

$$T_f e^{-\alpha_1 \lambda_1^2 t_2''} = \frac{T_f e^{-\alpha_1 \lambda_1^2 t_2'}}{e}$$

or

$$\alpha_1 \lambda_1^2 t_2'' = \alpha_1 \lambda_1^2 t_2' + 1$$

then

$$\lambda_1 = \sqrt{\frac{1}{\alpha_1 (t_2''-t_2')}} \qquad (32)$$

Now that the value of the eigenvalue λ_1 is known from the temperature history at $x=x_2$, the value of the thermal contact resistance can be determined from

equation (23),

$$R = \frac{\cot \lambda_1 x_1}{k_1 \lambda_1} + \frac{1}{k_2 \lambda_1} \sqrt{\frac{\alpha_2}{\alpha_1}} \cot \left(\lambda_1 \sqrt{\frac{\alpha_1}{\alpha_2}} x_2 \right) .$$

III. EXPERIMENTAL METHOD

A. Method Conforming to Analysis

The mathematical model developed previously demands that heat flow through the materials to be tested be one-dimensional. This requirement was met by uniformly irradiating the exterior surface, $x=-x_1$, as shown in Figure 5, with an instantaneous, uniformly distributed light pulse.

Also it was assumed during the mathematical analysis that the thermal properties, the thermal conductivity and the thermal diffusivity, and the thermal contact resistance are independent of temperature for the small temperature increases.

The associated boundary conditions used to solve the one-dimensional time-dependent heat transfer equation require that the specimens be thermally insulated after the initial impulse of radiant energy. In order for the exterior surfaces, at $x=-x_1$ and $x=x_2$, and the sides of the specimens to be adiabatic, the environment around the specimens was kept at low temperature and vacuum environment. The low temperature environment is required to reduce the effect of radiation heat losses from the specimens and a vacuum environment

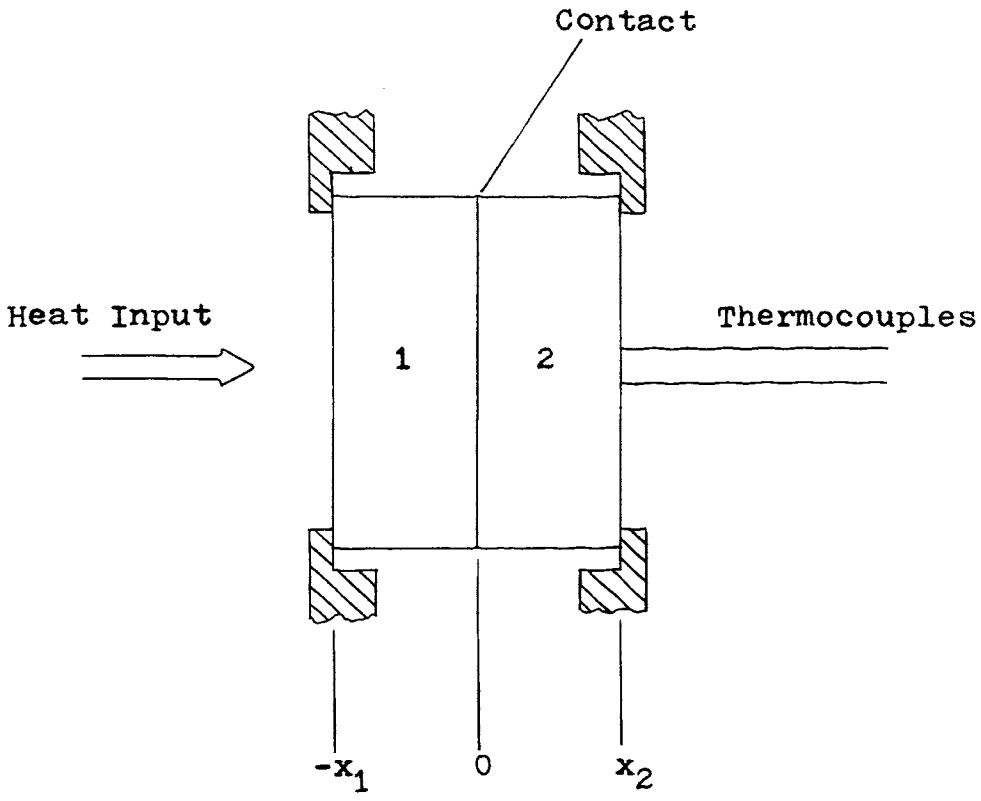

Heat Input to Specimens

Figure 5

reduces the convective mode of heat loss. The temperature of the specimens and the immediate surroundings was kept at approximately -10°F. The vacuum environment was approximately 10 microns to reduce effects of any possible heat losses due to free convection.

B. Description of Apparatus

The apparatus and test specimens used in the experimental analysis are shown in Figures 6 and 7. A schematic of the apparatus is shown in Figure 8.

In order to provide a vacuum environment for the experiments a stainless steel plate was made with several feed-throughs. Two feed-throughs were provided in order to facilitate the measurement of the degree of vacuum. One of the feed-throughs was connected by means of vacuum rubber tubing to a Virtis McLeod vacuum gage. A thermocouple vacuum gage was connected directly to the second feed-through opening in the vacuum plate.

The test fixture and specimen mounting fixture are shown in Figures 9 and 10 and also a schematic of the mounting fixture is given in Figure 11. The specimens were held together in contact by means of two plexiglass mounts of relatively low thermal

conductivity and were used to transmit the applied load to the specimens. The temperature of the of the plexiglass mounts was monitored by four copper-constantan thermocouples, a potentiometer, and an electronic ice point cell for a reference temperature.

On the rear surface of specimen 2, at $x=x_2$, a bismuth-telluride thermocouple, Bi_2Te_3, p and n pin, was spring loaded against the surface which provided means of measuring changes in temperature at position $x=x_2$. The thermocouple had a sensitivity output of 360uV/^{o}C at 0^{o}C. The two pins of the thermocouple were positioned about one-half inch apart. The separation of the thermocouple resulted in the measurement of the actual surface temperature at $x=x_2$. The thermocouple was also mounted in a copper block to assure uniform temperatures in the leads.

Two feed-throughs were provided for the copper-constantan thermocouples, the bismuth-telluride thermocouples, and ground wires. Also a feed-through in the base plate was provided for connection to a mechanical vacuum pump.

Three stainless steel pipes were welded to and below the vacuum plate through which thermocouple leads and threaded rods were accessible. To the ends of the pipes a stainless steel flange was welded which

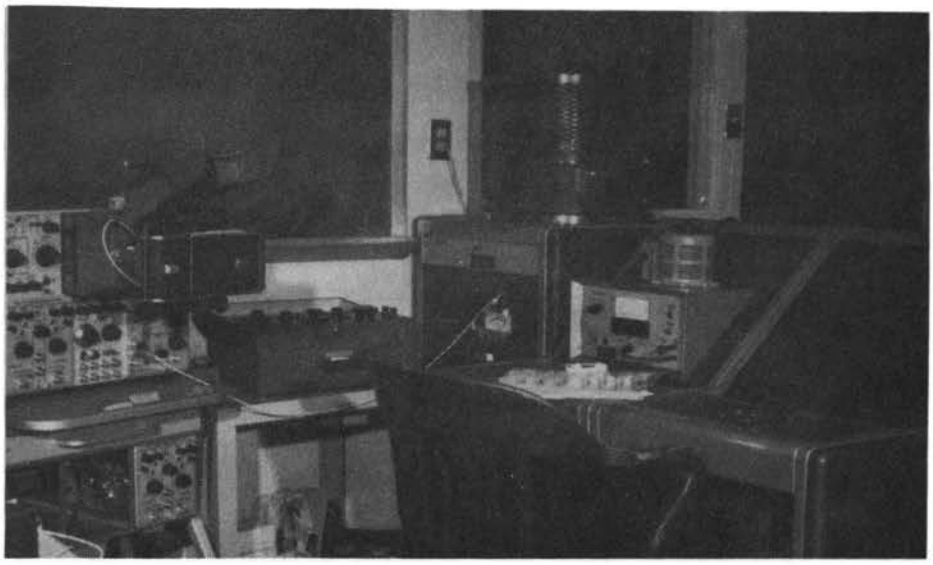

Equipment Arrangement

Figure 6

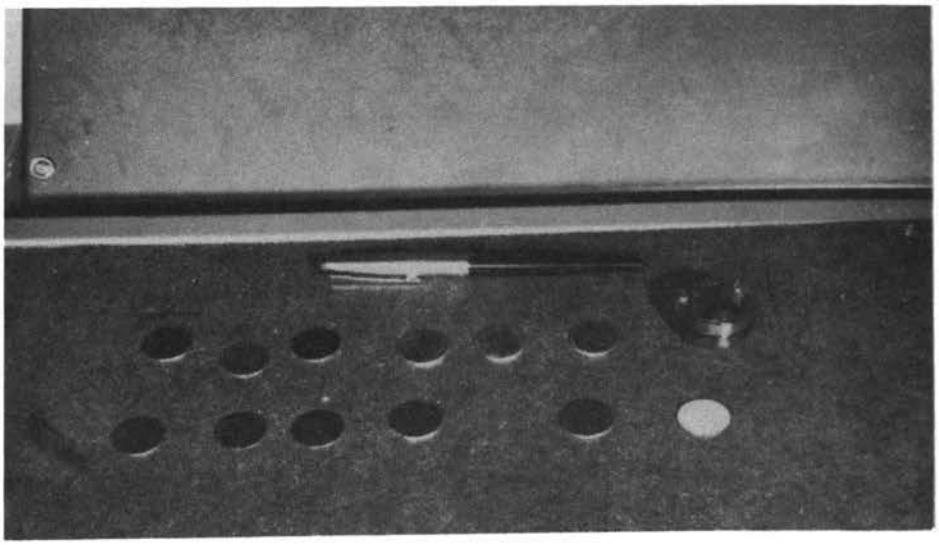

Test Specimens

Figure 7

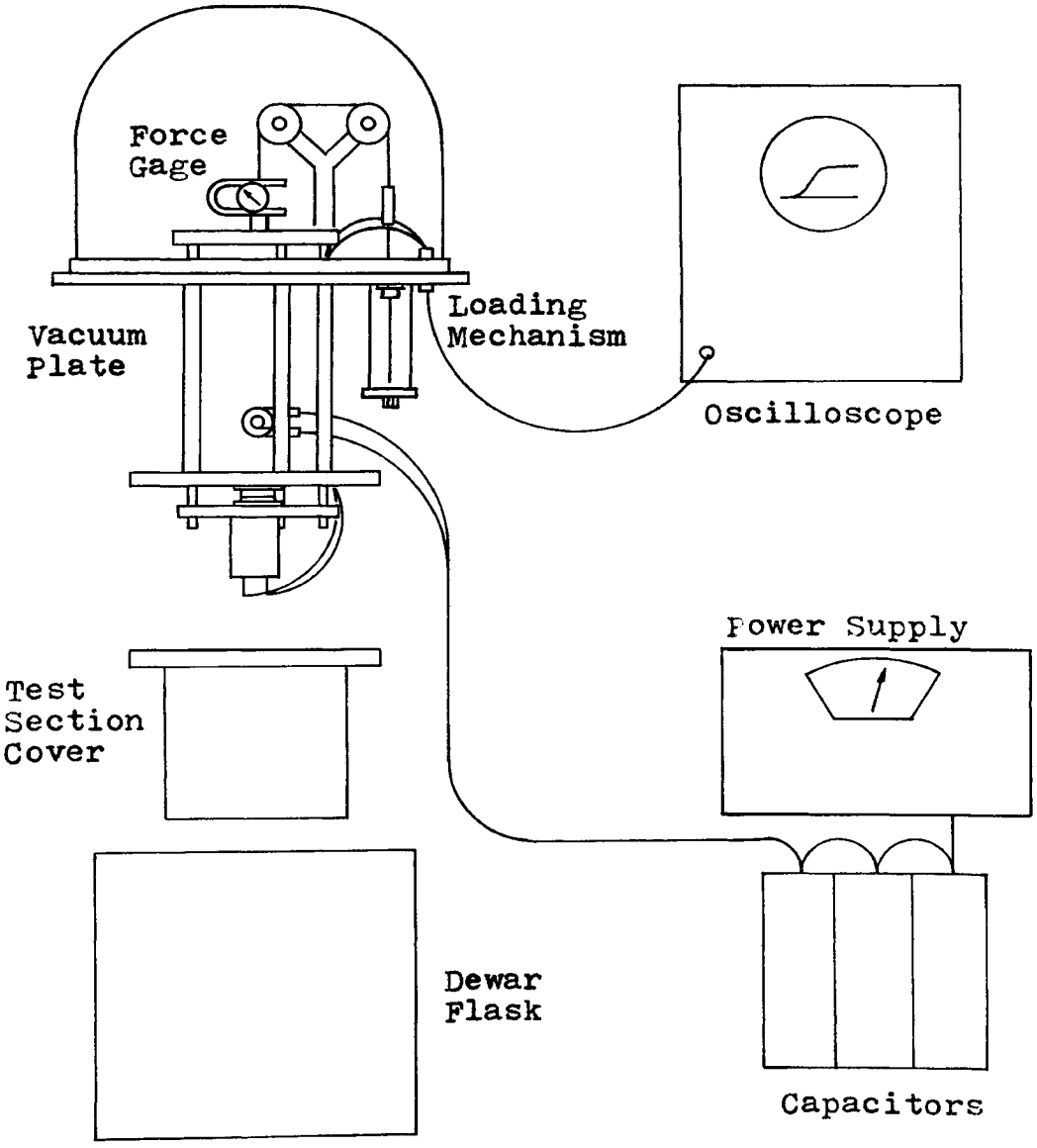

Schematic Diagram of Apparatus

Figure 8

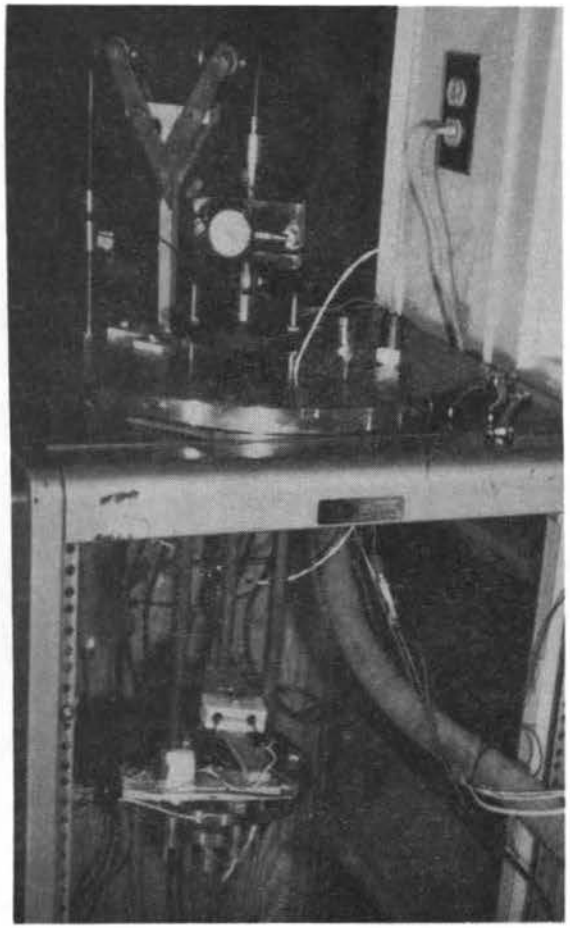

Test Fixture

Figure 9

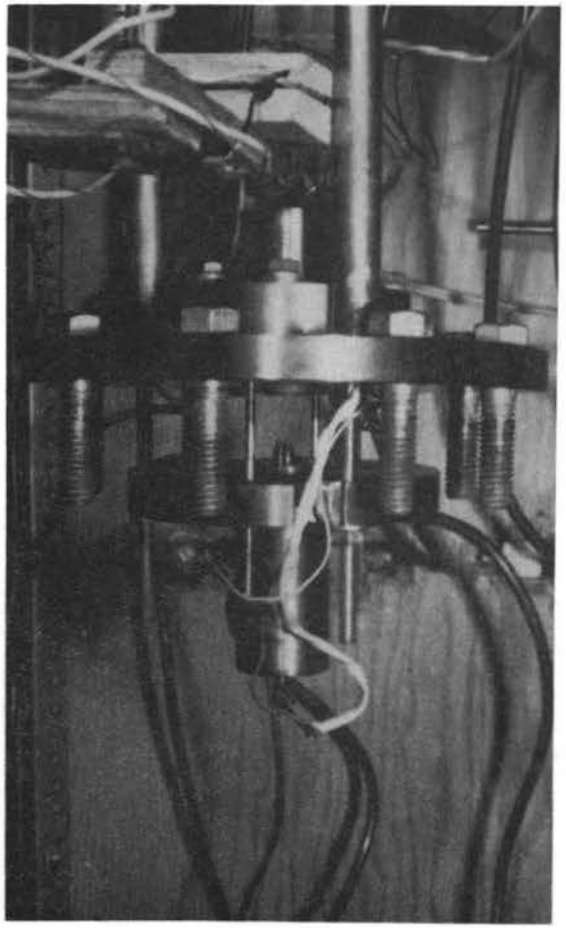

Specimen Mounting Fixture

Figure 10

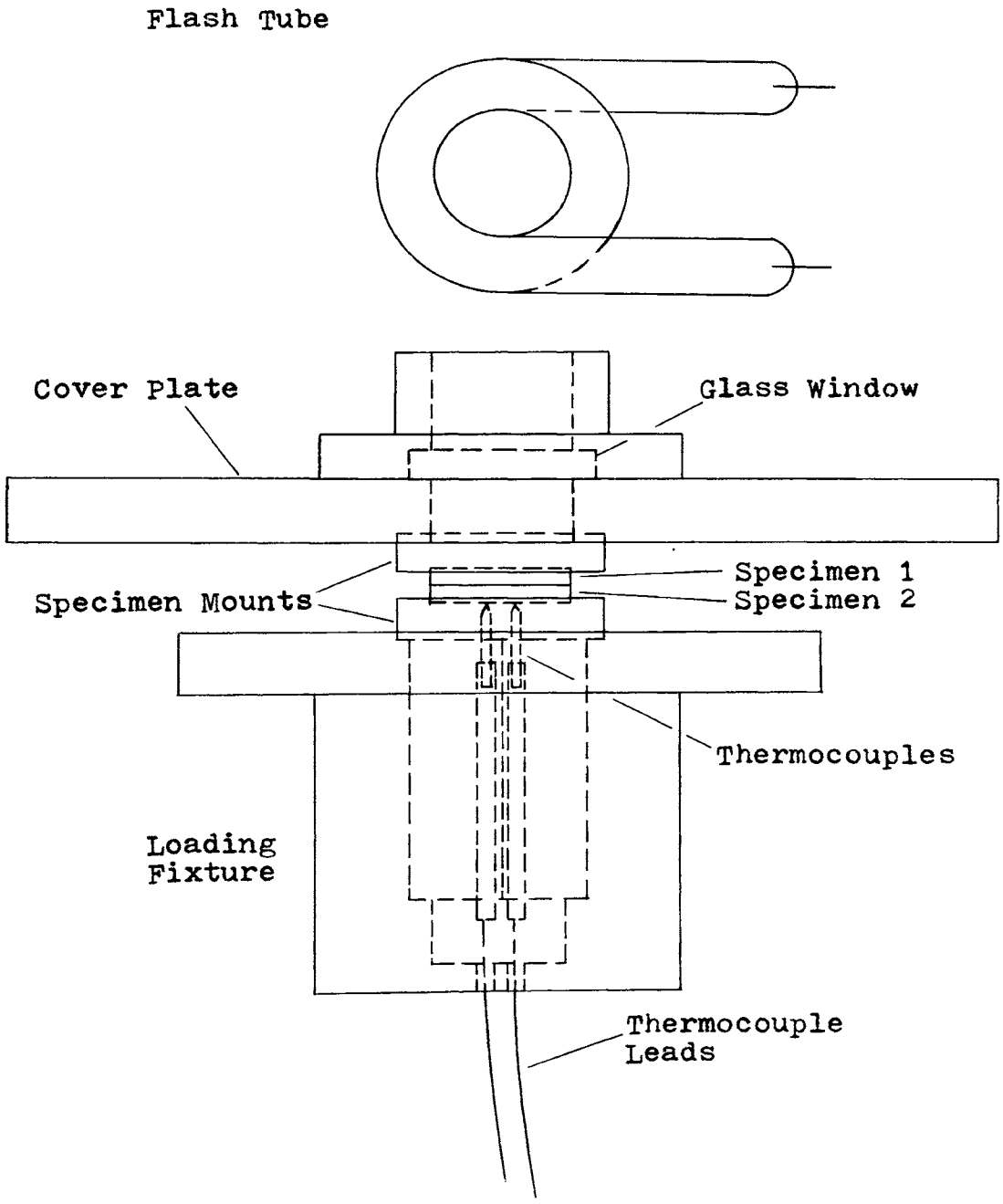

Schematic of Mounting Fixture

Figure 11

provided for a stainless steel cover to be bolted to the flange to facilitate a vacuum seal. A holder, as shown in Figure 10, for the copper blocks and bismuth-telluride thermocouple was mounted on the threaded rods extending through the pipes.

At the opposite end above the vacuum plate the threaded rods were attached to a plate to which a force gage, 0-100 pounds, was mounted. The force gage was attached to a steel cable by set screws and the cable diverted back to the vacuum plate over two pulleys. The cable then was connected to a steel rod by means of set screws and the steel rod attached to a small bellows mounted on the vacuum plate. A threaded rod was screwed through the bellows and with a pipe and nut arrangement allowed the application of the load to the specimens as shown in Figure 8.

A bell jar was used to enclose the upper surface of the vacuum plate.

The shielded leads from the bismuth-telluride thermocouple were connected to a Tektronix 1A7A plug-in amplifier, with a sensitivity of 10uV/cm, and a Tektronix type 556 Dual Beam oscilloscope. A Polaroid-Land camera was provided to record temperature-time curves obtained from the oscilloscope.

A pyrex window was placed over the specimens through which the heat impulse was provided by a

high-voltage flash tube, Amglo quarts HXQ-0312. An Amglo AC5000-1 power supply was used to charge the flash tube to 3000 volts and then discharge the flash tube by means of a high-voltage trigger.

To provide the low-temperature environment the lower flanged cover was immersed in liquid nitrogen which was placed in a large Dewar flask.

C. Description of Specimens

Test specimens were aluminum 2024-T3, aluminum 6061-T6, aluminum 7075-T6, copper 110, stainless steel 304, molybdenum and Armco iron. All test specimens were cut from round bar stock metals and machined to .788 inches in diameter. Parker, et al (27), suggested that for diffusivity measurements using a flash technique, specimens having thermal diffusivity of less than .2 Sq Cm/Sec (.772 Sq Ft/Hr) should be approximately 1 mm (.0394 inches) thick and for higher thermal diffusivities the specimens should be 3 mm (.118 inches) thick.

These guidelines were used when practical in preparing specimens for both thermal diffusivity and thermal contact resistance experiments. Thermal diffusivity experiments were performed to verify that the test equipment was operating properly for use

in the thermal contact resistance tests. The description of the theory, test set-up, results, and comparison to other results of the preliminary tests on the specimens for values of thermal diffusivity is discussed in Appendix A.

It is required for thermal diffusivity measurements that the duration of the heat input (from the flash tube) must be short compared to the time that the temperature rises on the back side of the specimen. Specimens that are too thin, as stated by Parker, et al, result in thermal diffusivities that are too low and if specimens are too thick the heat losses become more predominant.

Specimen thicknesses for the thermal contact resistance experiments were approximately .0394 inches for steel and iron specimens and .118 inches for aluminum, copper, and molybdenum specimens. The resulting composite of two specimens in contact resulted in a total thickness, from $-x_1$ to x_2, of approximately .0788 inches but kept at .118 inches for aluminum, copper and molybdenum specimens. Specimen dimensions are shown in Figure 12. The rise time of the temperature on the back surface of specimen two in general was on the order of .03 seconds and the flash duration approximately 1000 micro-seconds, so that the specimens were of sufficient thickness. Also since

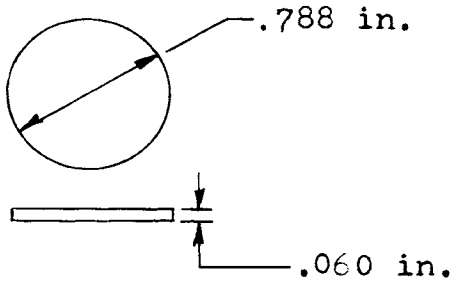

Nominal Dimensions for Aluminum, Copper, and Molybdenum Specimens

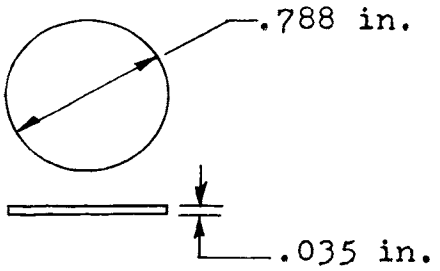

Nominal Dimensions for Stainless Steel and Armco Iron Specimens

Specimen Dimensions

Figure 12

most of the experiments, as described later, were in a vacuum and low temperature environment the heat losses from the specimens were negligible.

The values of the thermal diffusivity and thermal conductivity were assumed constant over the temperature ranges of the experiments and values of thermal conductivity were obtained from previously published data, (34) and (35). The values of thermal diffusivity were obtained from the measurements taken as described in Appendix A, at approximately $-10^{\circ}F$ and 10 microns vacuum. Physical dimensions and properties for each specimen as used in the experiments are listed in Appendix C.

All specimens were nominally flat as tested by a Zeiss Flatness Tester. All surfaces were polished with a 4/0 emory paper to obtain the nominally flat surface and to obtain surfaces as smooth as possible.

Surface roughnesses of the specimens were obtained by a profilometer, which consisted of a pilotor, amplimeter, and tracer. This instrument was capable of measuring rms (root-mean-square) and aa (arithmetic average) roughness of surfaces. Both measurements were made for all specimens on the contacting surface, at x=0. Also, standard Rockwell hardness tests were performed for all specimens. The resulting values

of rms and aa roughness and hardness with reference values for hardness are shown in Appendix C.

D. Experimental Procedure

1. Specimen and Equipment Preparation

After each specimen was polished and checked to be nominally flat at the contacting surfaces they were cleaned with acetone. The surface of the upper specimen, exposed to the heat flux from the flash tube, was coated with a thin layer of flat black paint to increase the energy absorbed from the flash tube. The lower test specimen, along with the painted specimen, was then placed in the plexiglass holders, shown in Figure 13, situated below the flash tube, separated by the pyrex glass window. The two bismuth-telluride thermocouples were placed against the back side of specimen 2. With no applied load the zero position was set on the Dillon force gage.

The cover for the specimens, specimen fixtures, and thermocouples were then bolted in place to the lower cover plate. The bell jar was placed on the vacuum plate and the vacuum pulled on the system to approximately 10 microns

(10^{-5}mm Hg), as determined by the McLeod gage.

The Dewar flask was positioned under the lower cover and was filled with liquid nitrogen. The cover and flask are shown in Figures 14 and 15.

The desired load for the test was obtained by turning the nut on the steel rod extending below the vacuum plate. The temperature of the plexiglass fixtures was measured using copper-constantan thermocouples which closely approximate the temperature of the specimens.

2. Test Procedure and Data Collection

After the desired apparent contact pressure, specimen temperature, and vacuum were obtained, the flash tube power supply was charged to approximately 3000 volts. After the oscilloscope was adjusted, normally to the .1mV/cm sensitivity, the trigger circuit for the flash tube was fired, discharging the capacitors through the flash tube. The setting of 3000 volts on the power supply yielded a discharge from the flash tube that gave a reasonable temperature rise on the back surface of specimen 2 within the sensitivity of the amplifier and oscilloscope.

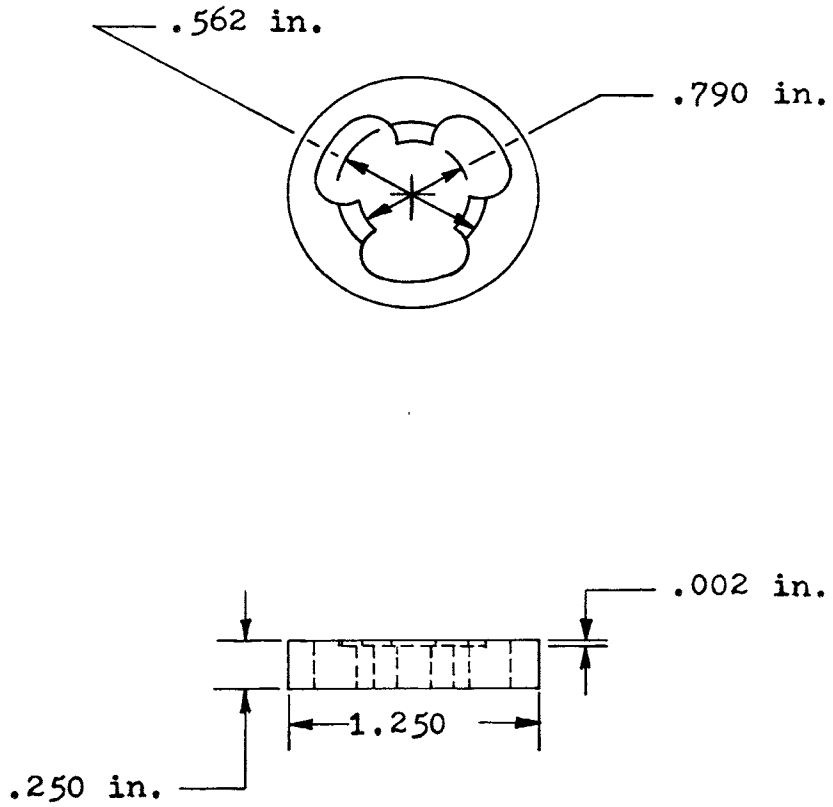

Specimen Mounts

Figure 13

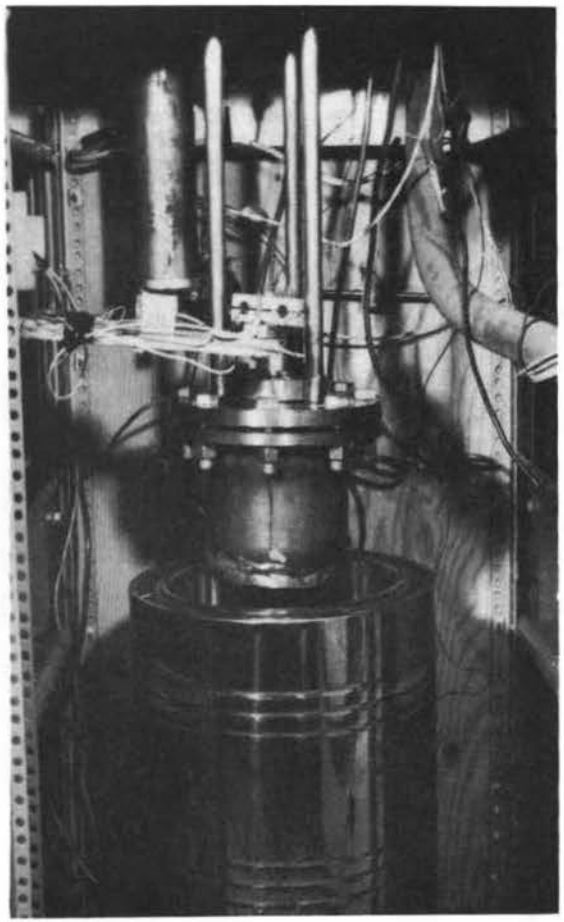

Lower Test Section

Figure 14

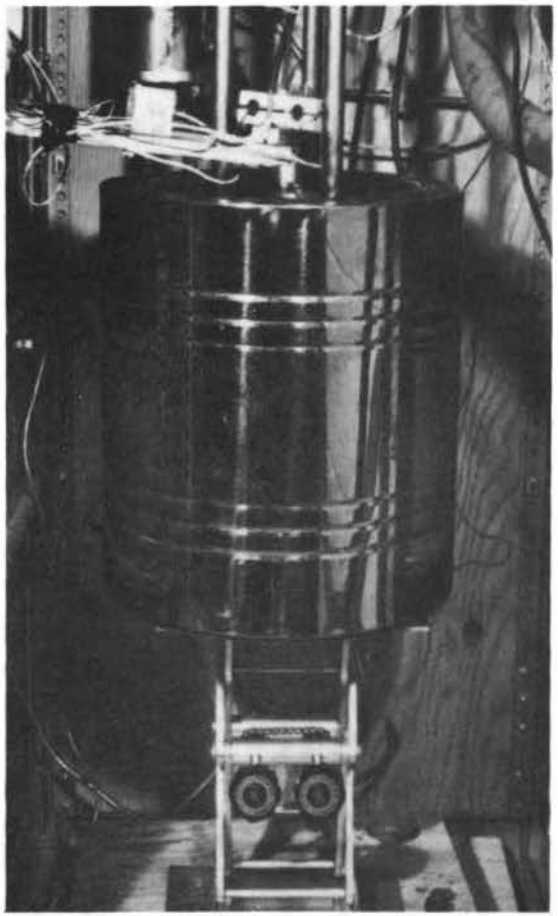

Dewar Flask in Position

Figure 15

In general the temperature rise was apprximately $1^{o}C$.

After the flash tube discharged the temperature history on the back surface of specimen 2, at $x=x_2$, was recorded from the oscilloscope by use of a Polaroid- Land camera.

The recording of the temperature rise was then used to calculate the thermal contact resistance.

Further tests on a single specimen pair only required the changing of the contact load.

3. Description of Experimental Series

After the initial thermal diffusivity measurements were made, experiments were performed on all specimen pairs to determine the variation of contact resistance with increasing contact pressure. This series of experiments was performed from 10 to 60 pounds of apparent load at 10 pound increments which corresponds to 20.7 psi to 124.2 psi for aluminum 2024-T3, aluminum 6061-T6, aluminum 7075-T6, copper 110, molybdenum, stainless steel 304, and Armco iron. The time delay between applying the load and the recording of data was approximately five minutes.

The aluminum 7075-T6 specimens were then used to determine the variation of thermal contact resistance with time after loading. The aluminum 7075-T6 specimens were loaded to an apparent contact pressure of 103.5 psi and data were taken at elapsed times of 2 minutes, 6 minutes, 10 minutes, 15 minutes, 30 minutes, 1 hour, 2 hours, and 4 hours.

The last series of experiments was performed to determine whether there was any directional effects for heat flow between specimens of different materials in contact. Aluminum 7075-T6 and copper 110 pairs were run at apparent contact pressures of 41.4, 82.8, and 124.2 psi.

The same experiment was performed on aluminum 6061-T6 and copper 110 pairs. A plexiglass mount that screwed together was used to hold the specimens in a fixed position and then placed in the loading fixture. The plexiglass holder allowed the specimens and the corresponding direction of heat flow to be reversed without disturbing their relative surface positions.

E. Data Reduction

From the millivolt output versus time curve, obtained at the rear surface of specimen 2, $x=x_2$, from the Polaroid print, the thermal contact resistance was determined.

As detailed in Figure 16, a time t_2' was picked a short time after the initial temperature rise, usually between .2 and 1 second for convenience. The corresponding temperature T_2' and then $\Delta T_2' = T_f - T_2'$ was calculated. The value for $\Delta T_2'' = \frac{\Delta T_2'}{e}$ was calculated and the corresponding value of T_2'' was found. This temperature (millivolt reading) corresponds to the time t_2''. The value for λ_1 was then calculated by the equation

$$\lambda_1 = \sqrt{\frac{3600}{\alpha_1(t_2''-t_2')}} \quad .$$

The contact resistance was then calculated using the equation, as before,

$$R = \frac{\cot \lambda_1 x_1}{k_1 \lambda_1} + \frac{1}{k_2 \lambda_1}\sqrt{\frac{\alpha_2}{\alpha_1}} \cot\left(\lambda_1\sqrt{\frac{\alpha_1}{\alpha_2}}\, x_2\right)$$

where x_1 = thickness of specimen 1, Ft

x_2 = thickness of specimen 2, Ft

α_1 = thermal diffusivity of specimen 1, Sq Ft/Hr

α_2 = thermal diffusivity of specimen 2, Sq Ft/Hr

k_1 = thermal conductivity of specimen 1, Btu/Hr Ft F

k_2 = thermal conductivity of specimen 2, Btu/Hr Ft F

λ_1 = eigenvalue, 1/Ft

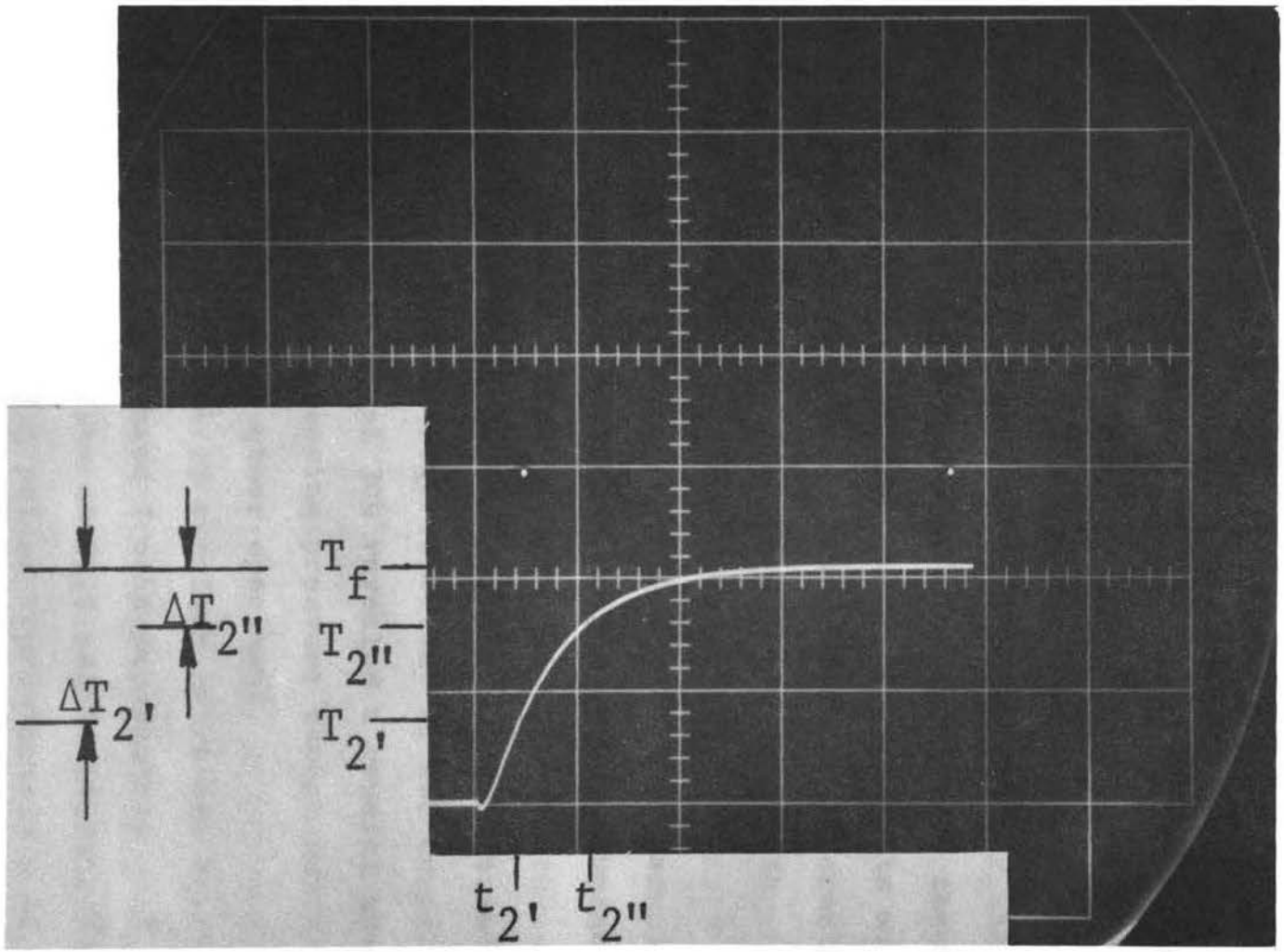

Typical Recording of Temperature History at $x=x_2$

Figure 16

IV. DISCUSSION AND RESULTS

A. Effect of Pressure

The initial series of experiments was performed to determine the effect of contact pressure on the thermal contact resistance. Since actual contact points are of a microscopic nature the greater the apparent contact pressure the greater will be the elastic and plastic deformation of these points at the contacting surfaces. Because of these deformations thermal contact resistance should decrease with increasing apparent contact pressure.

As shown in Figures 17 through 23 the thermal contact resistance decreased uniformly for aluminum 2024-T3, aluminum 6061-T6, aluminum 7075-T6, molybdenum, and Armco iron specimen pairs. Thermal contact resistance in Figures 20 and 21 for copper 110 and stainless steel 304 revealed a general trend to decrease with increasing pressure though not as uniformly as with the other specimens.

For aluminum 2024-T3 specimen pairs the thermal contact resistance ranged from approximately 24.7×10^{-4} Hr Sq Ft F/Btu at 20.7 psi to 14.2×10^{-4} Hr Sq Ft F/Btu at 103.5 psi or approximately a 42

percent decrease in thermal contact resistances.

Aluminum 6061-T6 specimen pairs resulted in thermal contact resistances from 21.65×10^{-4} Hr Sq Ft F/Btu at 20.7 psi to 12.93×10^{-4} Hr Sq Ft F/Btu at 124.2 psi apparent contact pressure. Aluminum 7075-T6 specimen pairs resulted in thermal contact resistances between 77.70×10^{-4} Hr Sq Ft F/Btu at 20.7 psi to 19.7×10^{-4} Hr Sq Ft F/Btu at 124.2 psi. These represent 40 percent and 75 percent decreases for aluminum 6061-T6 and 7075-T6 specimens, respectively.

Thermal contact resistances values for copper 110 ranged from 13.56×10^{-4} Hr Sq Ft F/Btu at 20.7 psi to 7.77×10^{-4} Hr Sq Ft F/Btu at 124.2 psi, a 43 percent decrease. Stainless steel thermal contact resistances varied from 152×10^{-4} Hr Sq Ft F/Btu to 117×10^{-4} Hr Sq Ft F/Btu from 20.7 psi to 124.4 psi apparent contact pressure, representing a 23 percent decrease.

Molybdenum specimen pairs resulted in thermal contact resistance values of 35.5×10^{-4} Hr Sq Ft F/Btu at 20.7 psi to 13.27×10^{-4} Hr Sq Ft F/Btu at 124.2 psi for approximately a 62 percent decrease. Armco iron specimen pairs resulted in thermal contact resistances of 130×10^{-4} Hr Sq Ft F/Btu at 124.2 psi

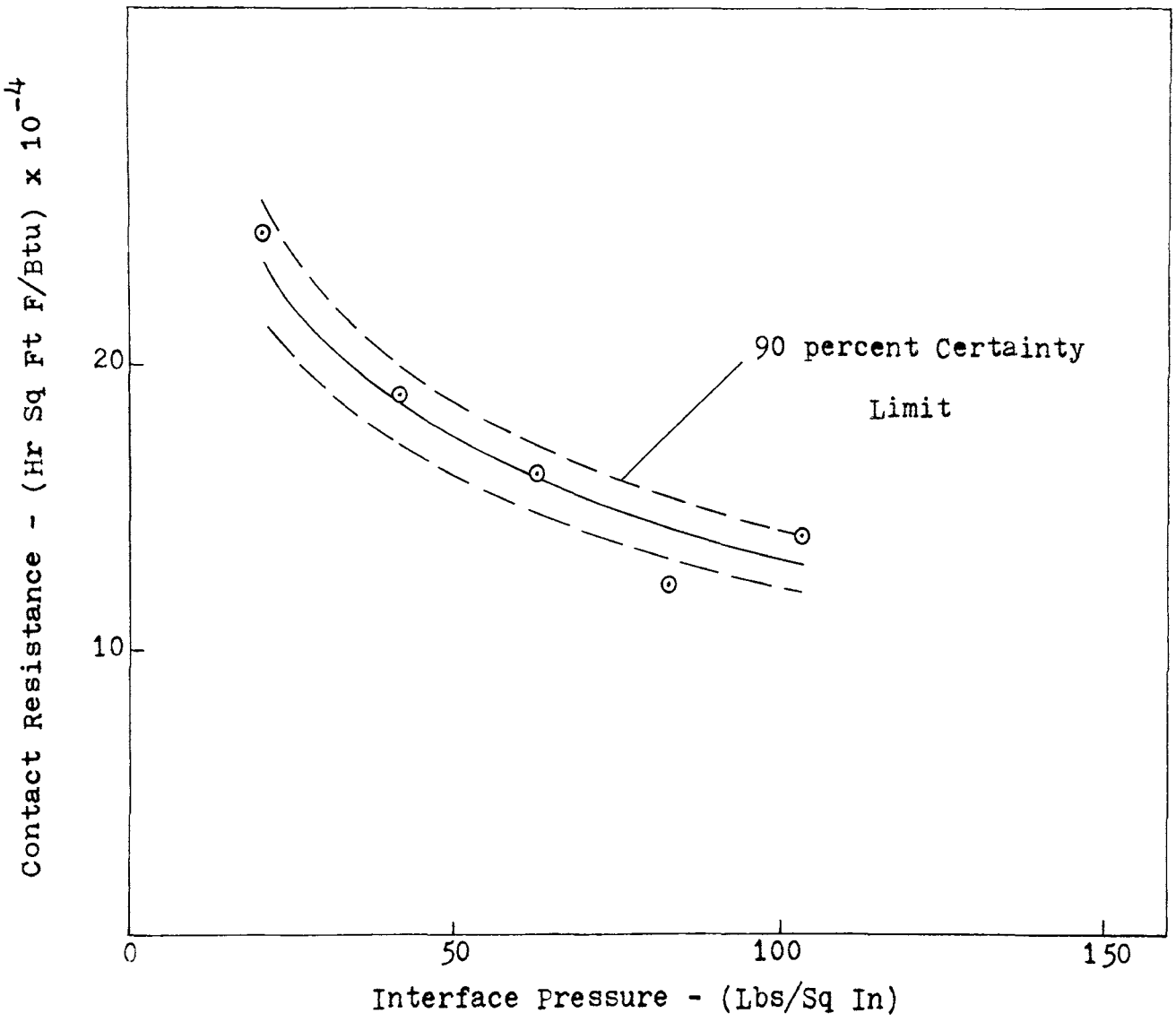

Thermal Contact Resistance for Aluminum 2024-T3
Figure 17

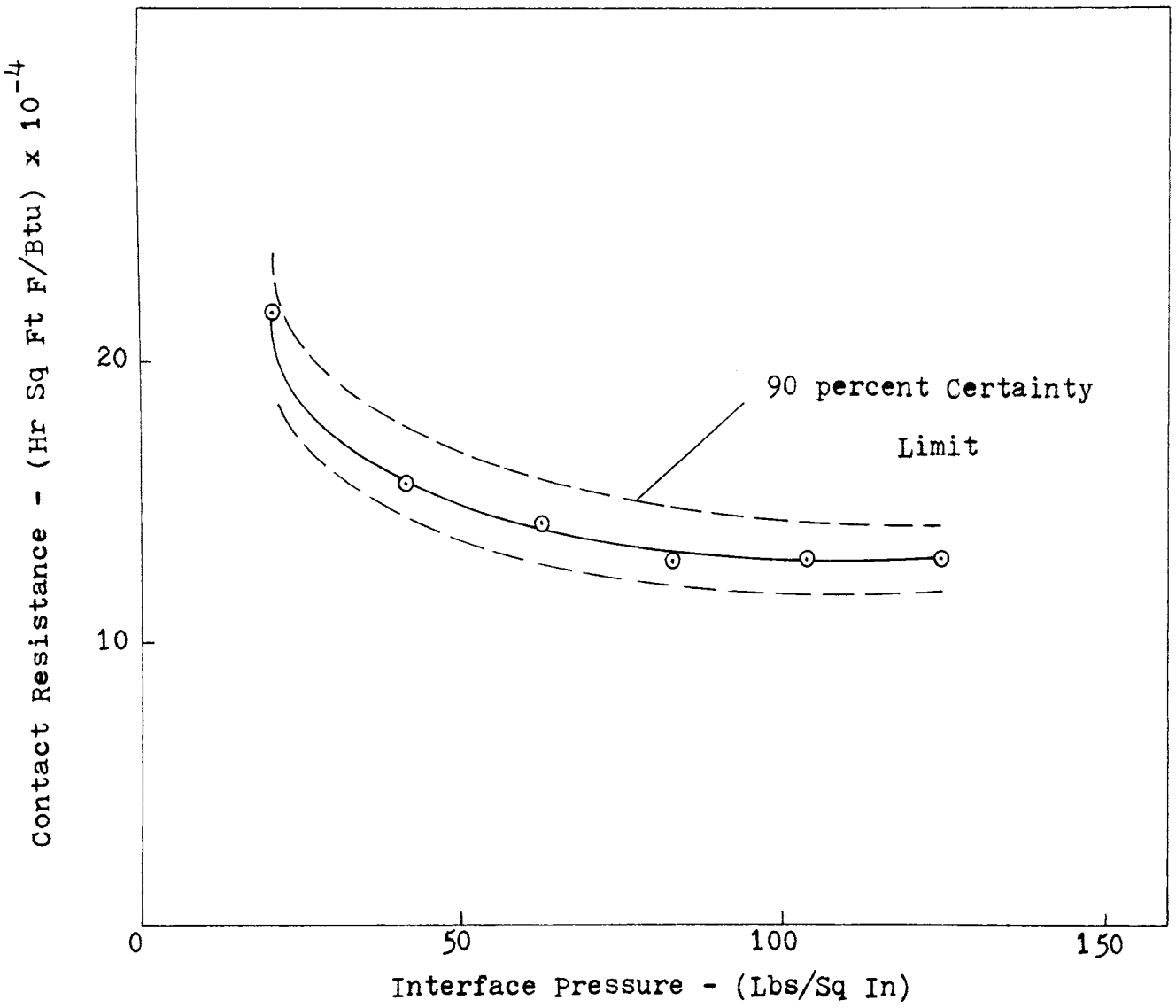

Thermal Contact Resistance for Aluminum 6061-T6

Figure 18

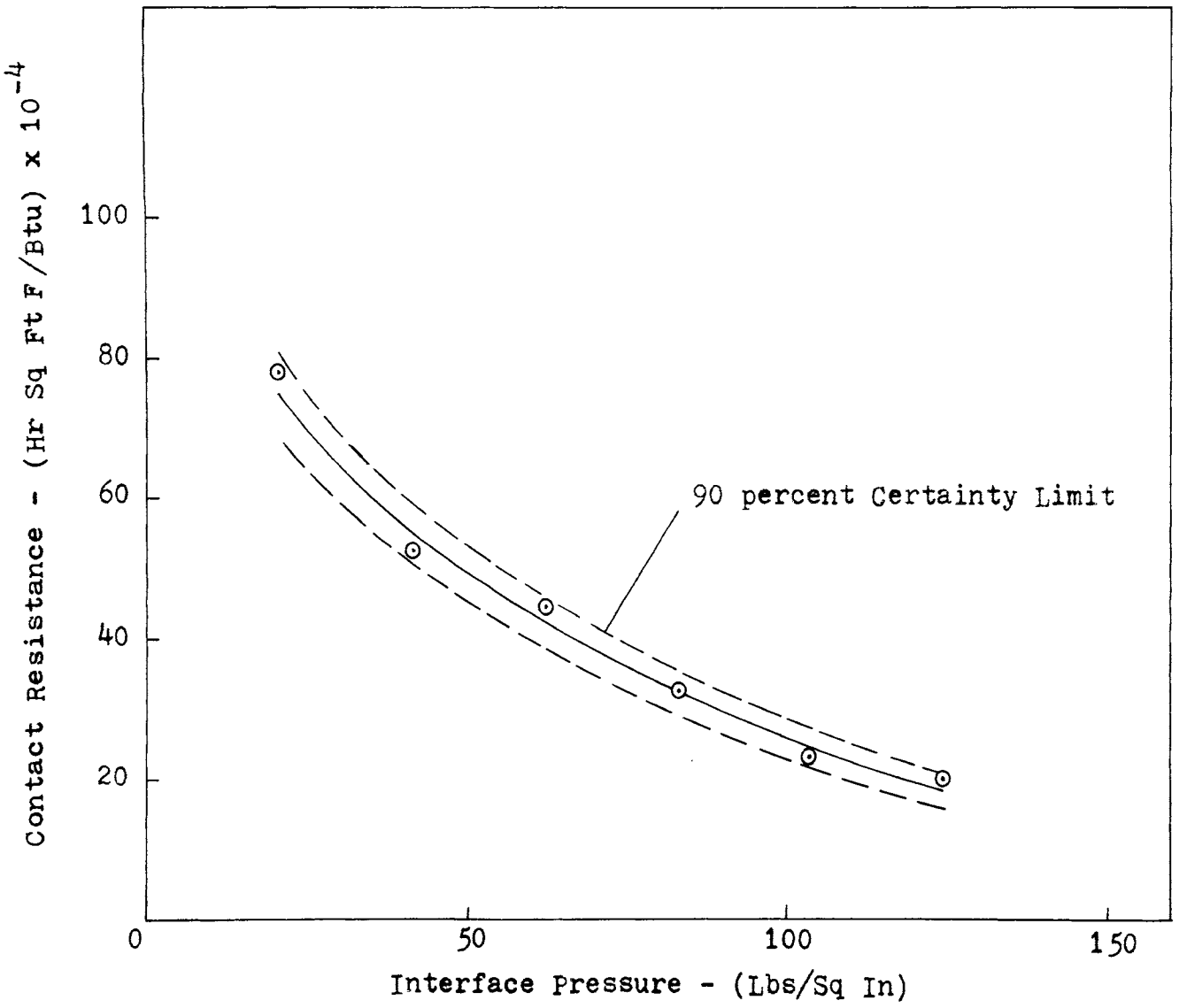

Thermal Contact Resistance for Aluminum 7075-T6

Figure 19

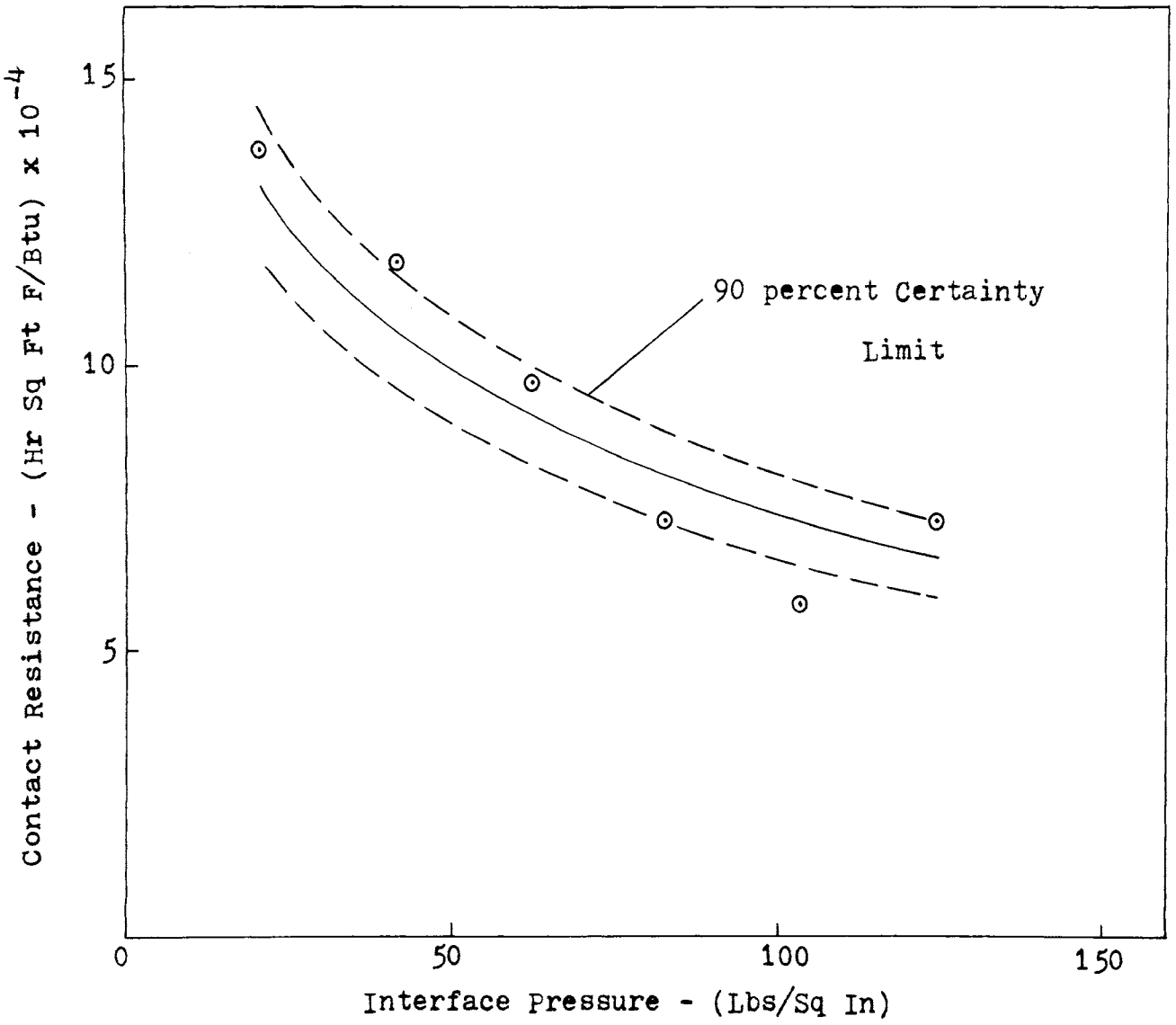

Thermal Contact Resistance for Copper 110

Figure 20

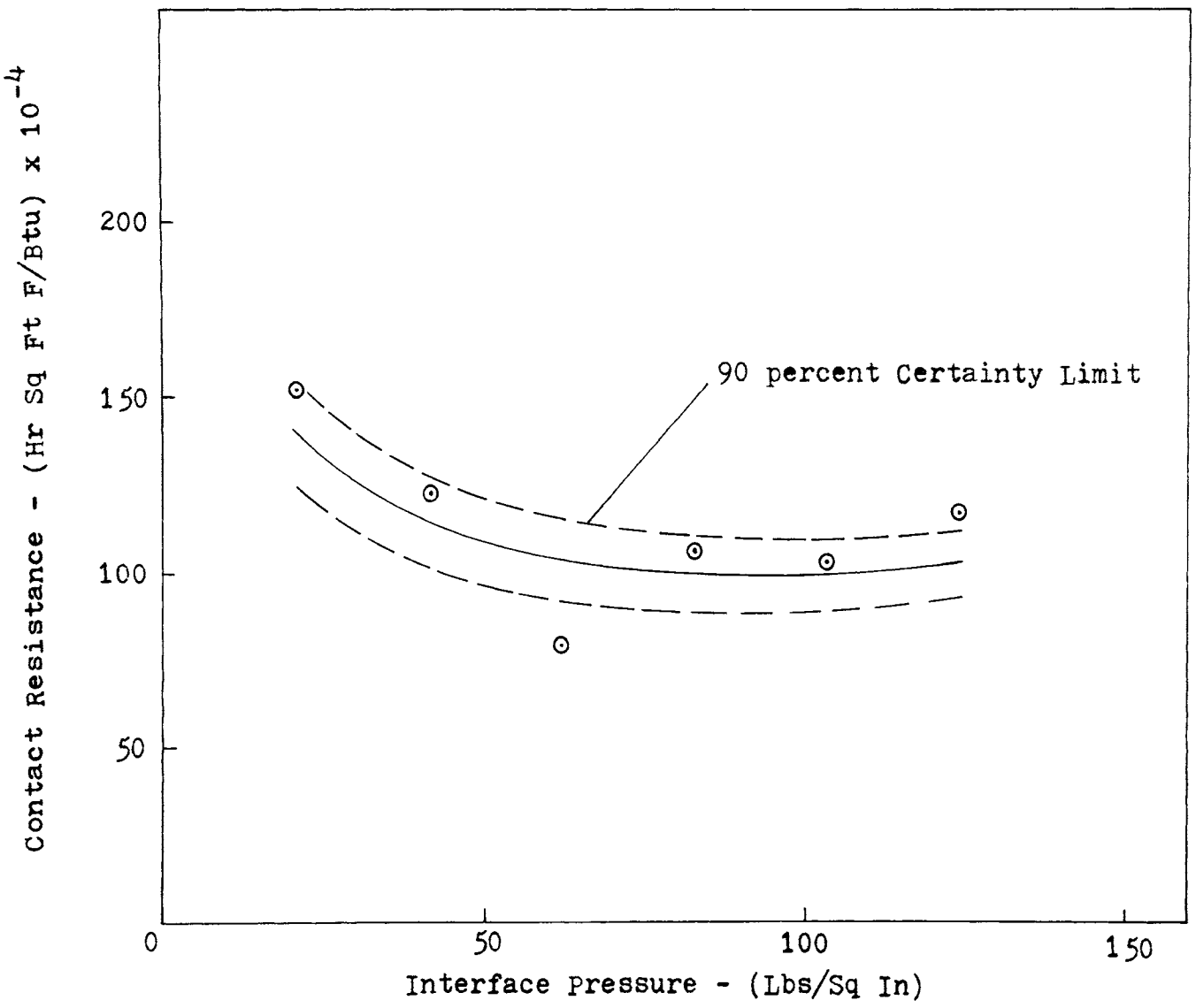

Thermal Contact Resistance for Stainless Steel 304

Figure 21

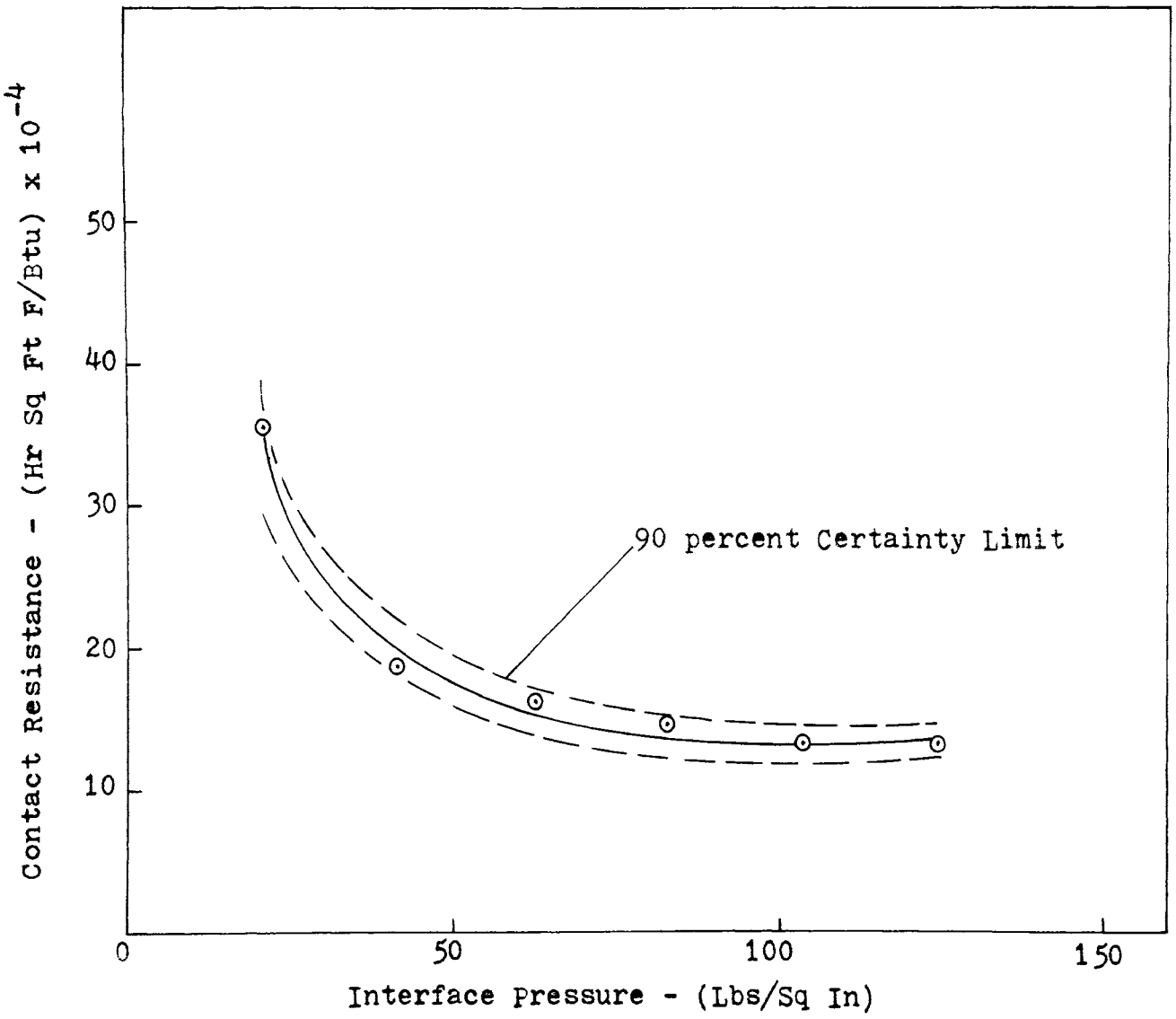

Thermal Contact Resistance for Molybdenum

Figure 22

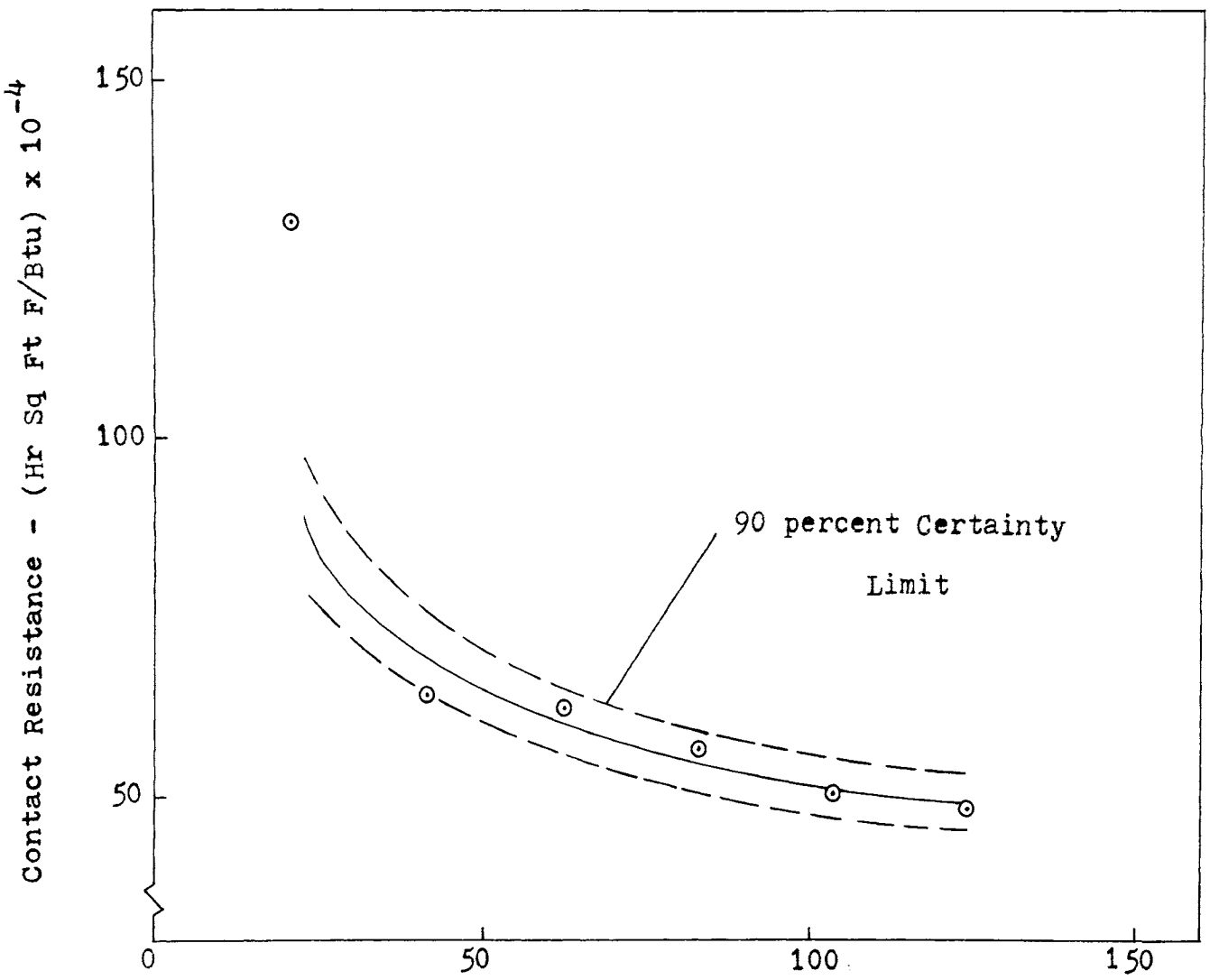

Thermal Contact Resistance for Armco Iron

Figure 23

which was a 63 percent decrease in thermal contact resistance.

B. Effect of Specimen Material

The specific type of material and the corresponding condition of the contacting surface determine the absolute value of the thermal contact resistance.

Surface hardness prescribes to what degree microscopic surface irregularities will deform to decrease the contact resistance by increasing the metal-to-metal contact area. From Rockwell B hardness measurements made on the specimens, as listed in Appendix C, the softer the material the more pronounced the effect of apparent contact pressure on thermal contact resistance.

From the aspect of surface hardness the thermal contact resistances for aluminum, molybdenum, and stainless steel specimens should be in the same relative range. Thermal contact resistances for copper and Armco iron should likewise be in the same relative range. As shown in Figures 17 through 23 and discussed in the previous section, absolute values of thermal contact resistances compare favorably for aluminum 2024-T3, aluminum 6061-T6, and molybdenum specimen pairs. Thermal contact resistance values for aluminum 7075-T6 and stainless steel 304 range above the other

specimens. Copper 110 thermal contact resistance values are noticeably lower than other material specimens but the values for Armco iron specimens more closely approximate values for aluminum 7075-T6.

C. Effect of Surface Conditions

The microscopic and macroscopic condition of the contacting surfaces determines to a large extent the actual values of thermal contact resistance. Due to the inherent inability to match contacting surfaces exactly as to flatness and surface roughness values of thermal contact resistance will vary accordingly.

All specimens were nominally flat as determined by a Zeiss flatness tester. The use of this tester though due to mounting limitations gives an indication of flatness only for the center region of the specimen. This as a result neglects the possibility of rounded corners as a result of polishing.

Through visual inspection the corners of most specimens seem to be flat within the limits of the flatness tester. The stainless steel specimens had visibly rounded corners as a result of polishing the surfaces. Also stainless steel tends to warp extensively when heated from machining. The thicknesses of the stainless steel specimens were approximately

.00292 and .00275 feet or .035 and .033 inches.

Due to these small thicknesses the stainless steel specimens could not be made to adhere to Parker, et al, (27) guidelines which would have made the specimens approximately .017 inches thick. Warpage at this thickness was quite dominant and even at thicknesses of .033 and .035 inches warpage of the contacting surfaces could have been a primary factor in large values of thermal contact resistances and a somewhat random trend with increasing pressure, as shown in Figure 21.

Surface roughnesses as measured by a Bendix Profilometer were approximately 2 micro-inches rms and aa as shown in Appendix C.

Previous work by Sauer, et al, (11) has shown that filler materials between the contacting surfaces such as silicone greases or aluminum foil greatly decrease the thermal contact resistance. This then establishes the concept of thermal contact resistances being directly dependent to a large degree upon the surface conditions.

D. Variation with Time

One of the primary uses of this transient technique was the ability to measure changes in thermal contact resistances with time after initial loading

of the specimens. Contacting surface irregularities tend to plastically deform after the applied load. This deformation then increases the actual contact area which results in decreasing the thermal contact resistance.

The results from the experiments on the aluminum 7075-T6 specimen pair are shown in Figure 25. After the initial load of 50 pounds (103.5 psi) was applied to the specimen the series of data were taken at varying intervals. The thermal contact resistance varied from 21.3×10^{-4} Hr Sq Ft F/Btu at 2 minutes (.0333 hour) elapsed time after loading and reached a constant value of 12.8×10^{-4} Hr Sq Ft F/Btu at 30 minutes with approximately the same value of contact resistance. This represented approximately a 40 percent decrease in thermal contact resistance.

Also shown in Figure 25 is the variation with time for the aluminum 7075-T6 specimen pairs with a constant load of 80 pounds (165.6 psi). The thermal contact resistance varied from 3.45×10^{-4} Hr Sq Ft F/Btu at 2 minutes (.0333 hour) elapsed time to 2.17×10^{-4} Hr Sq Ft F/Btu at 120 minutes (2.0 hours), representing a 37 percent decrease.

Similar experiments were performed on stainless steel 304 and copper 110, as shown in Figure 26.

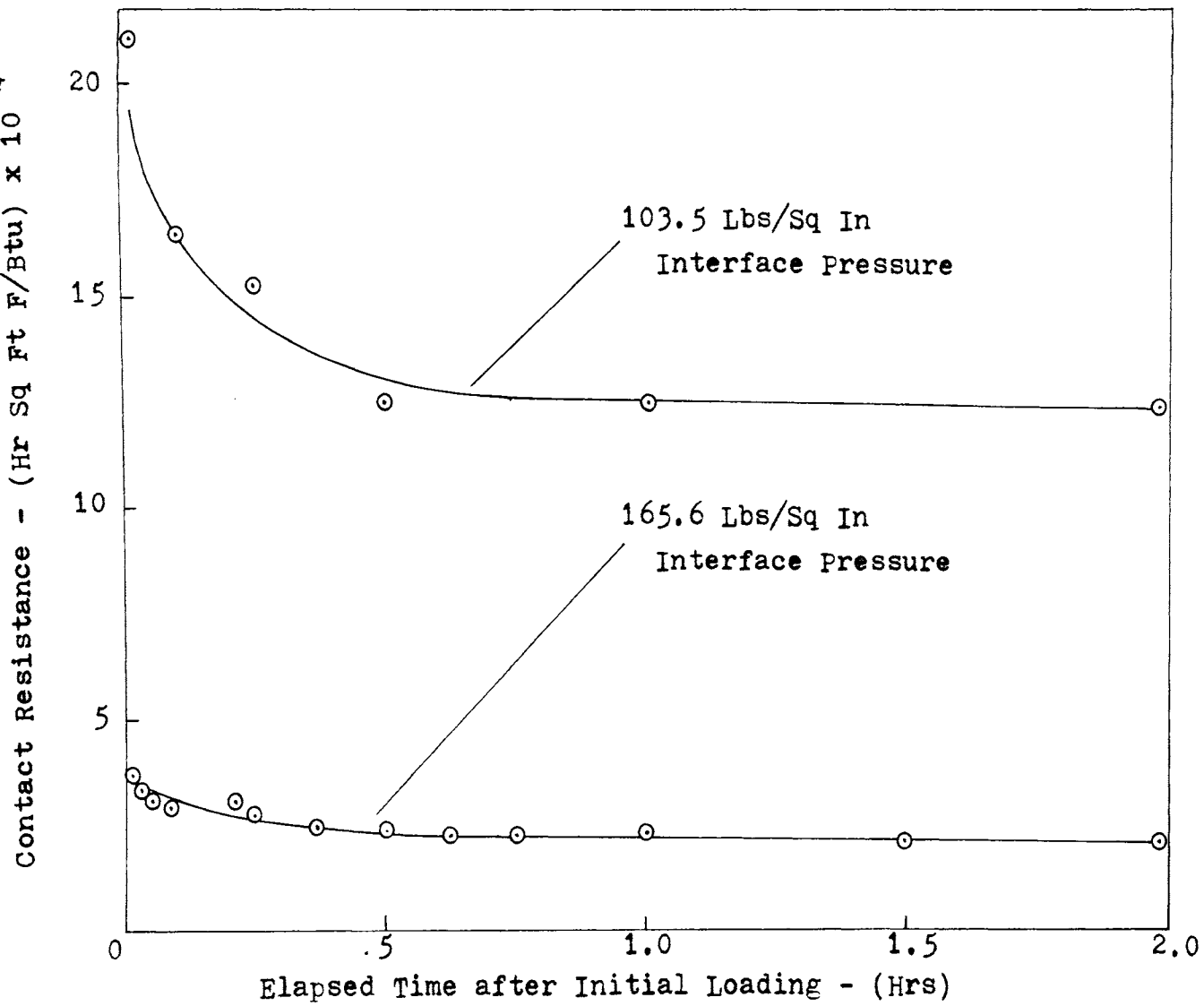

Variation of Thermal Contact Resistance with Time for Aluminum 7075-T6

Figure 24

Thermal contact resistances varied from 27.0×10^{-4} Hr Sq Ft F/Btu at 2.0 minutes (.016 hour) elapsed time to 22.0×10^{-4} Hr Sq Ft F/Btu at 120 minutes (2.0 hours) elapsed time for stainless steel 304 for a 9 percent decrease. Copper 110 specimens resulted in a change from 7.8×10^{-4} Hr Sq Ft F/Btu at 2.0 minutes (.016 hour) to 2.6×10^{-4} Hr Sq Ft F/Btu at 120 minutes (2.0 hours) elapsed time, representing a 66 percent decrease in thermal contact resistance.

From Figures 25 and 26 it can be seen that the thermal contact resistance changes significantly with time after initial loading and this fact should be considered in measurements of contact resistance.

E. Directional Effects

In previous investigations, primarily by Clausing and Chao (22) and later by Clausing (23) it was noted that there was a directional dependence upon the value of thermal contact resistance between two dissimilar metals as to the direction of heat flow.

One explanation of this discrepancy was put forth as microscopic curvature of the contacting

surfaces due to relatively high heat flow rates encountered in steady state methods of determining thermal contact resistance. High values of rates of heat flow were considered to be the cause due to differences in coefficients of thermal expansion of the two different materials. In the steady state method there usually exists large differences between the temperatures of the surfaces of the metals in contact.

The results of experiments using an aluminum 7075-T6 and copper 110 specimen pair and an aluminum 6061-T6 and copper 110 specimen pair are shown in Figure 27.

For the aluminum 7075-T6 and copper 110 specimen pair the thermal contact resistance varied from 11.11×10^{-4} Hr Sq Ft F/Btu at 41.1 psi to 9.68×10^{-4} Hr Sq Ft F/Btu at 124.2 psi contact pressure for heat flow from the aluminum specimen to the copper specimen.

When the specimens were inverted the corresponding values of thermal contact resistance varied between 7.83×10^{-4} Hr Sq Ft F/Btu at 41.4 psi and 9.19×10^{-4} Hr Sq Ft F/Btu at 82.8 psi.

Similarly for aluminum 6061-T6 and copper 110 specimen pair the thermal contact resistance ranged

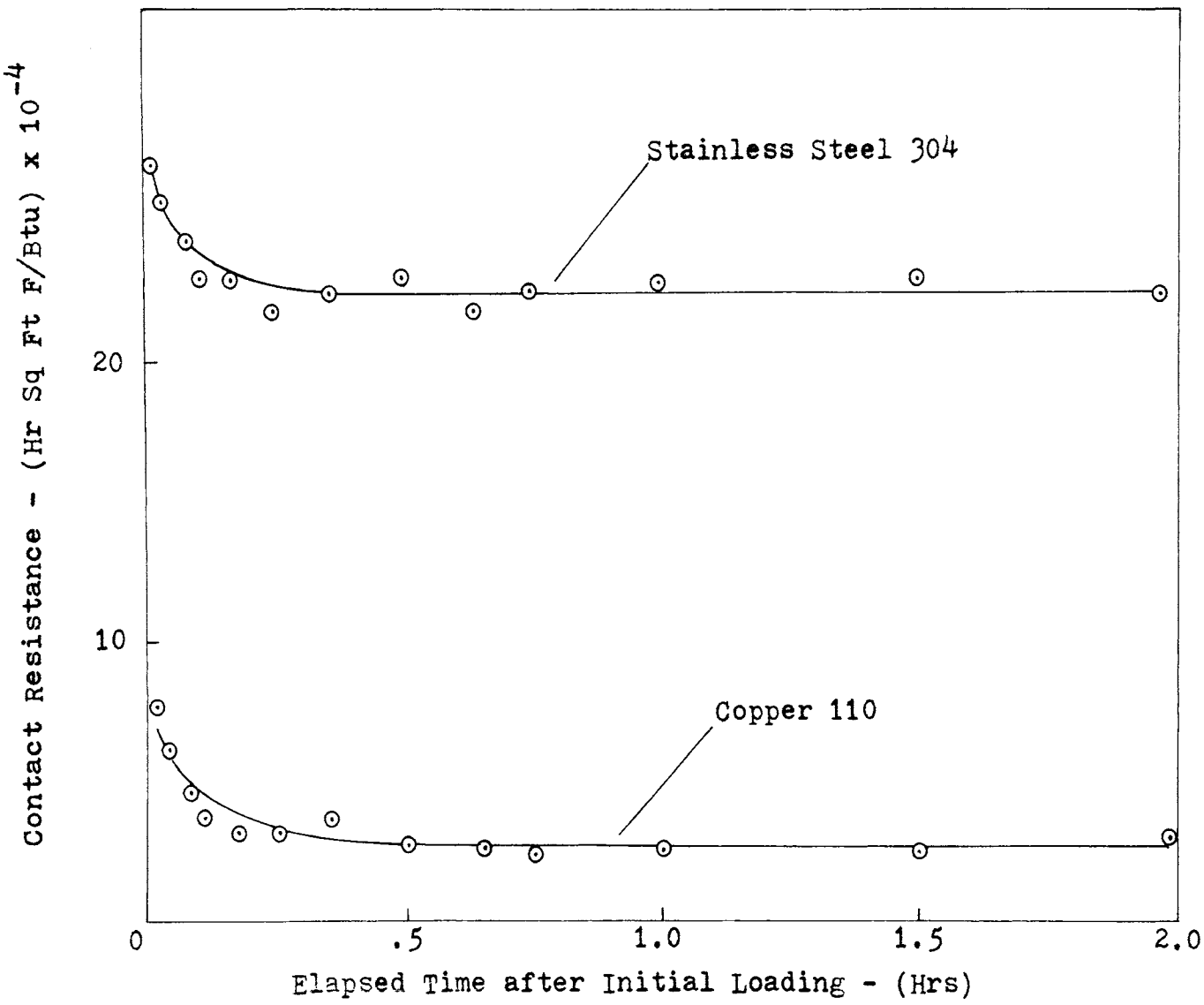

Variation of Thermal Contact Resistance with Time for Stainless Steel and Copper

Figure 25

from 6.92×10^{-4} Hr Sq Ft F/Btu to 5.65×10^{-4} Hr Sq Ft F/Btu at 41.4 psi to 124.4 psi contact pressures. The corresponding values of thermal contact resistance for heat flow of the copper 110 specimen to the aluminum 6061-T6 specimen ranged from 5.51×10^{-4} Hr Sq Ft F/Btu to 4.85×10^{-4} Hr Sq Ft F/Btu for the same pressure range.

These measurements resulted from only a few degrees temperature difference at the interface of the contacting surfaces. Since the two surfaces were kept in the same relative arrangement during the tests there is a definite directional effect.

Lewis and Perkins (25) attributed the directional dependence to the surface roughness and flatness. They found that the directional effect either increased or decreased depending upon the condition of the contacting surfaces, such that the degree of directional effect is dependent upon the surface conditions. It was also noted that at low interface pressure there was no noticeable directional effect.

Thomas and Probert (26) also attributed their experimental directional effects on differential thermal expansion. As with Lewis and Perkins, their results showed that contact resistance was lower when heat flowed from the specimen of higher thermal

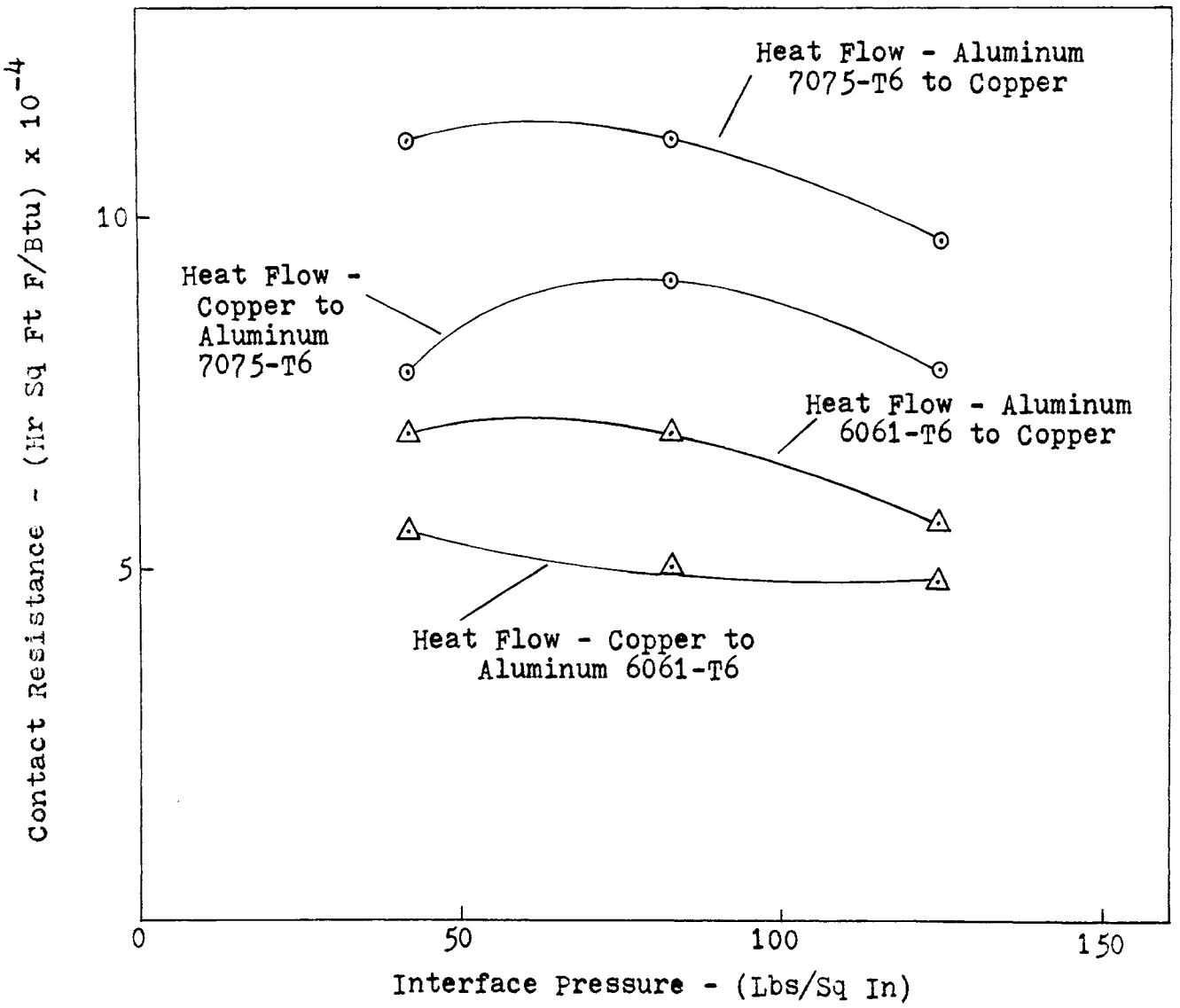

Directional Effects of Thermal Contact Resistance for Aluminum 7075-T6 and Copper

Figure 26

conductivity to the specimen of lower thermal conductivity.

The actual cause of directional effects remains unknown.

As shown in Figure 27, the contact resistance is less for heat flow from specimens of higher thermal conductivity to specimens of lower thermal conductivity. This then is in agreement with previous experiments.

The experimental conditions of lower interface temperature differential and relatively small apparent interface contact pressure appears to negate the theories of differential thermal expansion and lack of directional effects at small interface pressures.

F. Correlation of Data

Some previous efforts have been made to correlate published experimental results of thermal contact resistance. One such correlation by Thomas and Probert (19) compiles data from several sources for aluminum contacts. They proposed a correlation between a dimensional conductance or resistance, $R^* = sk/R$, where s is the surface roughness, k is the thermal conductivity, and R is the thermal contact resistance, and a dimensionless load, $W^* = W/(s)^2M$ where W is

the applied load and M is the surface hardness.

A computer program was written to establish a correlation between the work of Thomas and Probert and the aluminum experimental data represented in Figures 17 through 19 for aluminum specimens 2024-T3, 6061-T6, and 7075-T6.

As shown in Figure 27 a close correlation exists for all three specimens. The correlation by Thomas and Probert was made for machined interface surfaces and for smooth, polished surfaces as in this investigation. The thermal contact resistance was shown to be slightly less as verified by Figure 27.

In order to fit smooth curves to sets of data points the number of points usually must be much greater than the order of the approximating equation. Since quadratic and cubic least squares approximations did not approximate the points in Figures 16 through 26 a first order least squares line was approximated to the points after plotting the points on a semi-log scale.

These approximations were then replotted on the figures to obtain the given curves. Certainty limits of approximately 90 percent were provided for the curves shown in Figures 17 through 23, utilizing a method described by Kline and McClintock (36). This method is described in Appendix E.

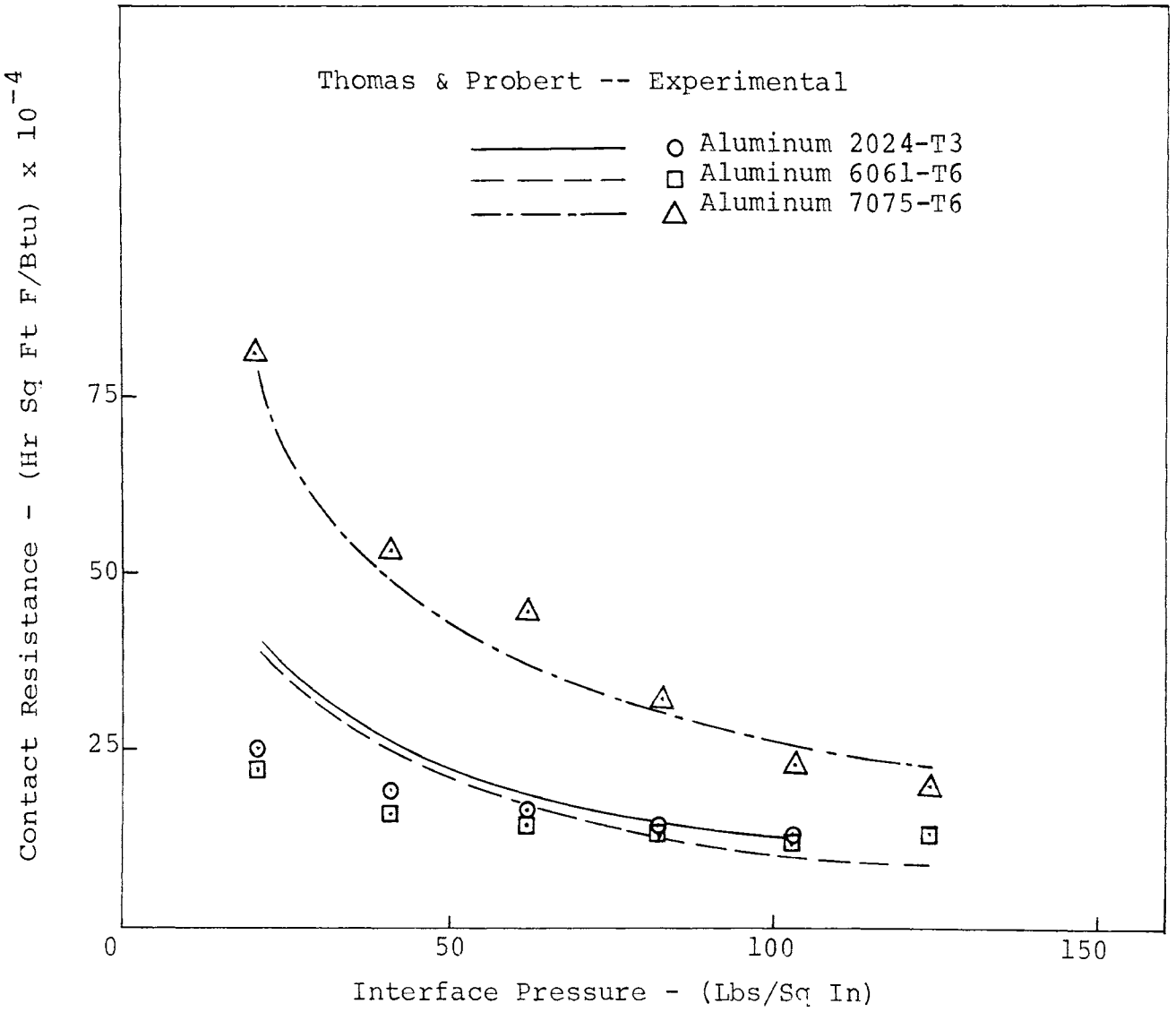

Correlation of Data for Aluminum Specimens
Figure 27

V. CONCLUSIONS

The experimental results of this investigation give rise to the following conclusions.

Increasing the apparent interface contact pressure decreases the thermal contact resistance. This was as expected since the microscopic surface irregularities will deform thereby increasing the actual contact area between the two specimens. Values for thermal contact resistances, for the materials and surface conditions described, ranged from approximately 152.0 Hr Sq Ft F/Btu at 20.7 psi for stainless steel 304 to 5.77 Hr Sq Ft F/Btu at 103.5 psi for copper 110. Decreases in thermal contact resistances were 42 percent for aluminum 2024-T3, 40 percent for aluminum 6061-T6, 75 percent for aluminum 7075-T6, 43 percent for copper 110, 23 percent for stainless steel 304, 62 percent for molybdenum, and 63 percent for Armco iron over the pressure range of 20.7 psi to 124.2 psi.

The pulse technique described was appropriately useful for measuring changes in thermal contact resistance over small time differentials after initial loading. Thermal contact resistances for

specimens of copper 110, stainless steel 304 at one constant interface pressure and aluminum 7075-T6 at two different interface pressures indicate a decrease of 35 to 50 percent from the initial time of loading until reaching a constant value.

The directional effect of thermal contact resistance variance as to the direction of heat flow between specimens of dissimilar thermal conductivities was shown not to be directly dependent upon differential thermal expansion. Also shown was that the phenomenon exists at relatively low interface pressures. Directional effects accounted for approximately a 20 percent difference in thermal contact resistance values over the pressure range tested.

Correlation of results to existing thermal contact resistance data was shown to agree very closely, especially as the interface pressure increased.

BIBLIOGRAPHY

1. Minges, M.L., "Thermal Contact Resistance," U.S.A.F. Report AFML-TR-65-375, Vol.1, 1966.
2. Fried, E., and Costello, F.A., "Interface Thermal Contact Resistance Problem in Space Vehicles," ARS Journal, Vol. 32, pp. 237-243, February 1962.
3. Fenech, H., and Rohsenow, W.M., "Prediction of Thermal Conductance of Metallic Surfaces in Contact," ASME J. Heat Transfer paper No. 62-HT-32, 1962.
4. Cetinkale, T.N., and Fishenden, M., "Thermal Conductance of Metals in Contact," General Discussion on Heat Transfer, Proceedings International Heat Transfer Conference, London, Institute of Mechanical Engineers, ASME, 1951, p.271.
5. Powell, R.W., "The Place of Heat Conduction in the Theory, Practice, and Testing of Bonds," Applied Materials Research, October 1962.
6. Petri, F.J., "An Experimental Investigation of Thermal Contact Resistance in a Vacuum," ASME Paper No. 63-WA-156, 1963.
7. Koh, B., and John, J.E.A., "The Effect of Interstitial Metallic Foils on Thermal Contact Resistance," ASME paper No. 65-HT-44, August 1965.
8. Barzelay, M.E., Tong, K.N., and Holloway, G., "Thermal Conductance of Contacts in Aircraft Joints," NACA TN 3167 (1954).

9. Barzelay, M.E., Tong, K.T., and Holloway, G.F., "Effect of Pressure on Thermal Conductance of Contact Joints," NACA TN 3295 (1955).

10. Fletcher, L.S., Smuda, P.A., and Gyorog, D.A., "Thermal Contact Resistance of Selected Low Conductance Interstitial Materials," AIAA paper No. 68-31, January 1968.

11. Sauer, H.J., Jr., Remington, C.R., Stewart, W.E., Jr., and Lin, J. T., "Thermal Contact Conductance with Several Interstitial Materials," Proceedings of the Eleventh International Thermal Conductivity Conference, Albuquerque, New Mexico, September 28- October 1, 1971.

12. Barzelay, M.E., and Holloway, G.F., "Effect of an Interface on Transient Temperature Distribution in Composite Aircraft Joints," NACA TN 3824 (1957).

13. Barzelay, M.E., "Range of Interface Thermal Conductance for Aircraft Joints," NASA TN D-426 (1960).

14. Shlykov, Yu.P., and Gamin, E.A., "Experimental Study of Contact Heat Exchange," RSIC-128, January 1964 (Redstone Scientific Information Center Report).

15. Thomas, T.R., and Probert, S.D., "Thermal Contact of Solids," Chemical and Process Engineering, November 1966, pp. 51-60.

16. Veziroglu, T.N., "Correlation of Thermal Contact Conductance Experimental Results," University of Miami Mechanical Engineering Report on NASA Grant NGR 10-007-010 1967.

17. Cooper, M.G., Mikic, B.B., and Yovanovich, M.M., "Thermal Contact Conductance," Int. J. Heat Mass Transfer, Vol. 12, pp. 279-300, 1969.

18. Holm, R., "Thermal Conduction through Nominally Flat Metallic Contacts in Vacuum Environment," Stackpole Carbon Co. Report, 1965.

19. Thomas, T.R., and Probert, S.D., "Correlations of Thermal Contact Conductance in Vacuo," ASME paper No. 71-HT-AA.

20. Mikic, B., and Carnasciali, G., "The Effect of Thermal Conductivity of Plating Material on Thermal Contact Resistance," ASME paper No. 69-WA/Ht-9, 1969.

21. Rogers, G.F.C., "Heat Transfer at the Interface of Dissimilar Metals," Int. J. Heat Mass Transfer, Vol. 2, pp. 150-154, 1961.

22. Clausing, A.M., and Chao, B.T., "Thermal Contact Resistance in a Vacuum Environment," J. Heat Transfer, Vol. 87, pp. 243-251, 1965.

23. Clausing, A.M., "Heat Transfer at the Interface of Dissimilar Metals - The Influence of Thermal Strain," Int. J. Heat Mass Transfer, Vol. 9, pp. 791-801, 1966.

24. Yovanovich, M.M., and Fenech, H., "Thermal Contact Conductance of a Nominally Flat, Rough Surface in a Vacuum Environment," AIAA paper 66-42 (1966).

25. Lewis, D.V., and Perkins, H.C., "Heat Transfer at the Interface of Stainless Steel and Aluminum - The Influence of Surface Conditions on the Directional

Effects," Int. J. Heat Mass Transfer, Vol.11, September 1968, pp. 1371-1383.

26. Thomas, T.R., and Probert, S.D., "Thermal Contact Resistance: The Directional Effect and Other Problems," Int. J. Heat Mass Transfer, Vol. 13, pp. 789-807, 1970.

27. Parker, W.J., Jenkins, R.J., Butler, C.P., and Abbott, G.L., "Flash Method of Determining Thermal Diffusivity, Heat Capacity and Thermal Conductivity," J. Applied Physics, Vol. 32, No. 9, pp. 1679-1684, September 1961.

28. Carslaw, H.S., and Jaeger, J.C., Conduction of Heat in Solids, Oxford University Press, New York, 2nd ed., 1959.

29. Cowan, R.D., "Pulse Method of Measuring Thermal Diffusivity at High Temperatures," J. Applied Physics, Vol. 34, No. 4, part 1, pp. 926-927, 1964.

30. Larson, K.B., and Koyana, K., "Measurement by the Flash Method of Thermal Diffusivity, Heat Capacity, and Thermal Conductivity in Two-Layer Composite Samples," J. Applied Physics, Vol. 39, No. 9, pp. 4408-4416, August 1968.

31. Danielson, G.C., "Specific Heat of High-Purity Iron by a Pulse-Heating Method," Semi-Annual Research Report in Physics, Ames Laboratory, ISL-901, pp. 16-19, 1957, Iowa State Laboratory.

32. Laurent, M.F., and Sauer, H.J.,Jr., "Transient Analysis of Thermal Contact Resistance," AIAA paper No. 71-438.

33. Moore, C.J., Jr., and Blum, H.A., "Heat Transfer Across Surfaces in Contact: Effects of Thermal Trnasients on One-Dimensional Composite Slabs," Proceedings of Seventh Thermal Conductivity Conference, Gaithersburg, Maryland, November 1967.

34. Materials in Design Engineering, Materials Selector Issue, Reinhold Publishing Corp., N.Y., October 1963.

35. Smithsonian Physical Tables, prepared by W.E. Forsythe, (The Smithsonian Institution, Washington, D.C., 1954), ninth revised edition.

36. Kline, S.J., and McClintock, F.A., "Describing Uncertainties in Single-Sample Experiments," Mech. Engr., 75 (January 1953), p. 3.

APPENDICES

APPENDIX A

THERMAL DIFFUSIVITY MEASUREMENT

1. Verification of Test Equipment

In order to verify that the test equipment used in this investigation was operating properly, several experiments were performed to measure the thermal diffusivity of the test specimens.

A similar flash technique was used by Parker, et al, (27) in determining the thermal diffusivity of several materials. Their application of an equation given by Carslaw and Jaeger (28) for the temperature distribution within a thermally insulated solid resulted in the following equation

$$\alpha = \frac{1.38L^2}{\pi^2 t_{\frac{1}{2}}} \qquad (A1)$$

where α = thermal diffusivity

x = thickness of test specimen

and $t_{\frac{1}{2}}$ = time duration from the discharge of the flash tube until the temperature at the back surface of the specimen reached one-half of its final value.

The temperature distribution at the rear surface,

x=L, opposite the flash tube, was given by

$$T(L,t) = \frac{Q}{DCL}\left(1+2\sum_{n=1}^{\infty}(-1)^n e^{-\left(\frac{-n^2\pi^2\alpha t}{L^2}\right)}\right) \qquad (A2)$$

where Q = energy of pulse from the flash tube

D = density of test specimen

C = heat capacity of specimen

The maximum temperature at the rear surface is then

$$T(L,\infty) = \frac{Q}{DCL} = Tm \ . \qquad (A3)$$

To non-dimensionalize this equation the terms V and W were defined as follows:

$$V(L,t) = T(L,t)/Tm \qquad (A4)$$

$$w = \frac{\pi^2\alpha t}{L^2} \qquad (A5)$$

Then

$$V = 1+2\sum_{n=1}^{\infty}(-1)^n e^{-(-n^2 w)} \qquad (A6)$$

When the temperature rise has reached one-half of its final value, or V = .5, the corresponding value of w is 1.38. Therefore , the thermal

diffusivity, can be derived as in equation (A1), or

$$\alpha = \frac{1.38L^2}{\pi^2 t_{\frac{1}{2}}}$$

Equation (A1) was used to verify that the equipment used to make the measurements during the thermal contact resistance experiments was operating properly.

Tables 1 and 2 show the results of these experiments with a comparison to the results obtained by Parker, et al, and other references for values of thermal diffusivity.

TABLE 1

THERMAL DIFFUSIVITY MEASUREMENTS

Material	$\alpha(\frac{cm^2}{sec})$ Measured *	$\alpha(\frac{cm^2}{sec})$ Parker, et al	$\alpha(\frac{cm^2}{sec})$ Other Sources	
Aluminum 2024-T3	.453	-	.742	(35)
Aluminum 6061-T6	.657	-	.653	(35)
Aluminum 7075-T6	.455	-	.45	(35)
Copper 110	1.045	1.07 - 1.15	1.14	(35,36)
Stainless Steel 304	.0377	-	.0404	(35)
Molybdenum	.403	-	.523	(35)
Armco Iron	.182	.18 - .19	.17	(36)

* Values given are representative of data taken, as shown in Table 2.

TABLE 2

THERMAL DIFFUSIVITY DATA

Specimen	$\alpha(\frac{cm^2}{sec})$
Aluminum 2024-T3	.45, .453, .453, .45
Aluminum 6061-T6	.648, .66, .657, .657
Aluminum 7075-T6	.464, .45, .455, .455
Copper 110	.93, 1.045, 1.045, 1.045
Stainless Steel 304	.0333, .035, .035, .035
Molybdenum	.405, .405, .402, .403, .403
Armco Iron	.165, .175, .165, .175, .175, .186, .193, .191

APPENDIX B

EXPERIMENTAL DATA

TABLE 3

THERMAL CONTACT RESISTANCE DATA FOR ALUMINUM

Specimens	Load (Lbs)	Contact Resistance $R(Hr\ SqFt\ F/Btu)^{x10^{-4}}$
Aluminum 2024-T3	10	24.70
	20	18.92
	30	16.23
	40	12.35
	50	14.20
Aluminum 6061-T6	10	21.65
	20	15.60
	30	14.25
	40	12.93
	50	12.93
	60	12.93
Aluminum 7075-T6	10	77.70
	20	52.20
	30	44.40
	40	32.30
	50	22.75
	60	19.70

TABLE 4

THERMAL CONTACT RESISTANCE DATA

FOR COPPER, STAINLESS STEEL, MOLYBDENUM, AND ARMCO IRON

Specimens	Load (Lbs)	Contact Resistance R(Hr SqFt F/Btu)x10^{-4}
Copper 110	10	13.56
	20	11.75
	30	9.73
	40	7.77
	50	5.77
	60	7.77
Stainless Steel 304	10	152.0
	20	125.5
	30	78.4
	40	106.3
	50	102.8
	60	117.0
Molybdenum	10	35.50
	20	18.65
	30	16.25
	40	14.50
	50	13.27
	60	13.27

Table 4 (continued)

Specimens	Load	Contact Resistance
Iron	10	130.3
	20	64.0
	30	62.2
	40	56.2
	50	50.2
	60	48.4

TABLE 5

THERMAL CONTACT RESISTANCE DATA

FOR VARIATION WITH TIME EXPERIMENTS

Specimen	Load (Lbs)	Elapsed Time (Hrs)	R (Hr SqFt F/Btu)x10^{-4}
Aluminum 7075-T6	50	.0333	21.3
		.11	16.9
		.25	15.4
		.5	12.8
		1.0	12.8
		2.0	12.8
Aluminum 7075-T6	80	.016	3.65
		.033	3.24
		.067	3.16
		.0825	2.97
		.16	3.07
		.25	2.90
		.33	2.77
		.5	2.67
		.67	2.67
		.75	2.70
		1.00	2.56
		1.50	2.40
		2.00	2.17

Table 5 (continued)

Specimen	Load	Elapsed Time	R (Hr SqFt F/Btu)x10^{-4}
Copper 110	80	.016	7.8
		.033	6.2
		.061	4.5
		.0825	3.5
		.16	3.0
		.25	3.0
		.33	3.4
		.5	2.5
		.67	2.5
		.75	2.2
		1.00	2.4
		1.50	2.2
		2.00	2.6
Stainless Steel 304	80	.016	27.0
		.033	25.6
		.061	24.3
		.0825	23.0
		.16	22.8
		.25	21.7
		.33	22.5
		.5	23.0
		.67	21.7
		.75	22.5
		1.00	22.7
		1.50	22.7

TABLE 6

THERMAL CONTACT RESISTANCE DATA

FOR DIRECTIONAL EFFECT EXPERIMENTS

Specimens	Load (Lbs)	R (Hr SqFt F/Btu)x10^{-4}
AL 7075-T6	20	11.11
to	40	11.11
Copper 110	60	9.68
Copper 110	20	7.83
to	40	9.19
AL 7075-T6	60	7.83
AL 6061-T6	20	6.92
to	40	6.92
Copper 110	60	5.65
Copper 110	20	5.51
to	40	5.05
AL 6061-T6	60	4.85

APPENDIX C

MATERIAL AND SPECIMEN PROPERTIES

TABLE 7

PHYSICAL DIMENSIONS AND VALUES OF MEASURED DIFFUSIVITY

All specimens .4835 in^2 in area.

Specimen	Diffusivity x(in)	Diffusivity $(\frac{ft^2}{hr})$	Contact Resistance x_1(ft)	Contact Resistance x_2(ft)
Aluminum 2024-T3	.1185	1.76	.00503	.00483
Aluminum 6061-T6	.121	2.54	.00503	.00475
Aluminum 7075-T6	.119	1.765	.00475	.00491
Copper 110	.118	4.05	.00508	.00500
Molybdenum	.060	1.565	.00500	.00475
Stainless Steel 304	.041	.146	.00292	.00275
Armco Iron	.039	.706	.00316	.00292

TABLE 8

SPECIMEN THERMAL CONDUCTIVITY, HARDNESS, SURFACE ROUGHNESS

Specimen	Thermal Conductivity (Btu/hr-ft-F)	Hardness Rockwell	Hardness Brinell	Roughness RMS ($in \times 10^{-6}$)
Aluminum 2024-T3	109.2	90	170	1.3 2.0
Aluminum 6061-T6	99.0	80	140	1.5 1.5
Aluminum 7075-T6	77.0	96.7	180	2.0 1.5
Copper 110	226.0	69.3	115	1.0 1.0
Molybdenum	84.5	94.5	190	2.0 2.0
Stainless Steel 304	9.4	87	160	2.0 2.0
Armco Iron	37.976	64.2	105	2.0 2.0

APPENDIX D

APPARATUS LIST

1. Power Supply - Amglo Model AC-5000 (0-5000 volts)
2. Capacitators - Amglo 50 MFD
3. Flash Tube - Amglo Model HXQ-0312
4. Vacuum Gages -
   a. Norton Thermocouple Vacuum Gage NRC 801
   b. Virtis McLeod Gage
5. Vacuum Pump - Welsh Scientific Model 1402
6. Force Gage - Dillon Force Gage, 0-100 lbs.
7. Reference Cell - Dynatech Ice Point Cell ($32^{\circ}F$)
8. Oscilloscope - Tektronix Type 556 Dual-Beam
9. Amplifier - Tektronix Type 1A7A High Gain Differential Amplifier, Plug-In, 10 micro-volts to 10 volts
10. Potentiometer - Honeywell Model 2745
11. Roughness Measure - Bendix Profilometer
12. Flatness Tester - Zeiss

APPENDIX E

UNCERTAINTY ANALYSIS

The following procedure for estimating the uncertainty of experimental results was described by Kline and McClintock (36).

The uncertainty w of an experimental observation R was defined in equation form as

$$w_R = \left(\left(\frac{\partial R}{\partial v_1} w_1\right)^2 + \left(\frac{\partial R}{\partial v_2} w_2\right)^2 + \cdots + \left(\frac{\partial R}{\partial v_n} w_n\right)^2\right)^{\frac{1}{2}}$$

where R is a function of n independent variables $v_1, v_2, \ldots, v_n$.

For this investigation R, the thermal contact resistance, was given previously as

$$R = \frac{\cot \lambda_1 x_1}{k_1 \lambda_1} + \frac{1}{k_2 \lambda_1} \frac{\alpha_2}{\alpha_1} \cot\left(\lambda_1 \frac{\alpha_1}{\alpha_2} x_2\right)$$

where the values of x_1, x_2, α_1, α_2, k_1, k_2, and λ_1 are the independent variables.

The uncertainties of x_1, x_2, α_1, α_2, k_1, k_2, and λ_1 corresponding to w_1 through w_7 were determined

from the probable experimental errors.

Then the uncertainty of R, the thermal contact resistance, is then

$$w_R = \left(\left(\frac{\partial R}{\partial x_1} w_1\right)^2 + \left(\frac{\partial R}{\partial x_2} w_2\right)^2 + \left(\frac{\partial R}{\partial \alpha_1} w_3\right)^2 + \left(\frac{\partial R}{\partial \alpha_2} w_4\right)^2 + \left(\frac{\partial R}{\partial k_1} w_5\right)^2 + \left(\frac{\partial R}{\partial k_2} w_6\right)^2 + \left(\frac{\partial R}{\partial \lambda_1} w_7\right)^2\right)^{\frac{1}{2}}$$

The error in measuring x_1 and x_2 was small compared to other variables and was considered negligible. The error in the values of $_1$ and $_2$ were considered to be a maximum of 5 percent. Maximum error for values of k_1 and k_2 was considered to be approximately 3 percent. Errors in calculating $_1$ were considered to be a maximum of 5 percent.

As an example in calculating a 90 percent certainty range for R for the aluminum 2024-T3 specimens at 20.7 psi interface pressure, the uncertainty, w, was

$$w_R = \left(2\left(\frac{.00247}{1.76} \times .088\right)^2 + 2\left(\frac{.00247}{109.2} \times 3.28\right)^2\right.$$

$$+ \left(\frac{.00247}{38.25} \times 1.91\right)^2)^{\frac{1}{2}}$$

$$= .000239 .$$

Then,

$$\frac{w_R}{R} = 9.67 \% .$$

VITA

William Edward Stewart, Jr. was born on November 5, 1944 in St. Louis, Missouri.

He attended Ritenour Senior High School in Overland, Missouri and graduated in June, 1963. In September, 1963 he entered the University of Missouri-Rolla, graduating with a Bachelor of Science degree in Mechanical Engineering in January, 1968 after completing a Cooperative Engineering student program with McDonnell - Douglas Corporation, St. Louis, Missouri.

In February, 1968 he entered graduate school at the University of Missouri - Rolla. From May, 1968 to September, 1969 he worked in industry at McDonnell - Douglas Corporation and Hussmann Refrigeration, also of St. Louis.

In September, 1969 he enrolled again as a graduate student in Mechanical Engineering obtaining his Master of Science degree in December, 1970.